

AD-A103 278

SACLANT ASW RESEARCH CENTRE LA SPEZIA (ITALY)

F/6 20/1

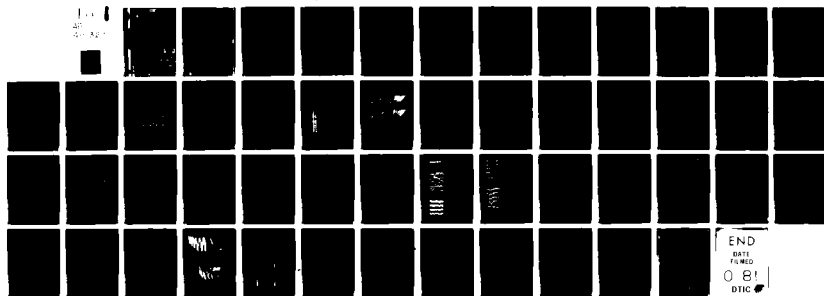
VARIABILITY OF ACOUSTIC TRANSMISSIONS IN A SHALLOW WATER AREA (U)

MAY 81 E SEVALDSEN

UNCLASSIFIED

SACLANTCEN-SR-46

NL

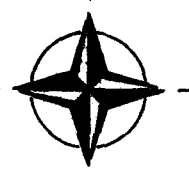


LEVEL

13

SACLANTCEN Report
SR-46 ✓

SACLANTCEN Report SR - 46



SACLANT ASW
RESEARCH CENTRE
REPORT

AD A103278

VARIABILITY OF ACOUSTIC TRANSMISSIONS IN A SHALLOW WATER AREA

by

ERIK SEVALDSEN

DTIC
ELECTE
AUG 25 1981
A

1 MAY 1981

This document has been approved
for public release and sales its
distribution is unlimited.

NORTH
ATLANTIC
TREATY
ORGANIZATION

This document is unclassified. The information it contains is published subject to the provisions of the
legend printed on the inside cover. Short quotations from it may be made in other publications if credit is
given to the author(s). Except for working copies for research purposes or for use in internal publications,
reproduction requires the authorization of the Director of SACLANTCEN.

FILE COPY

81 8 25 077

This document is released to a NATO Government at the direction of the SACLANTCEN subject to the following conditions:

1. The recipient NATO Government agrees to use its best endeavours to ensure that the information herein disclosed, whether or not it bears a security classification, is not dealt with in any manner (a) contrary to the intent of the provisions of the Charter of the Centre, or (b) prejudicial to the rights of the owner thereof to obtain patent, copyright, or other like statutory protection therefor.

2. If the technical information was originally released to the Centre by a NATO Government subject to restrictions clearly marked on this document the recipient NATO Government agrees to use its best endeavours to abide by the terms of the restrictions so imposed by the releasing Government.



14 SACLANTCEN ~~SECRET~~ SR-46

NORTH ATLANTIC TREATY ORGANIZATION

SACLANT ASW Research Centre

Viale San Bartolomeo 400, I-19026 San Bartolomeo (SP), Italy

tel: national 0187 560940
international + 39 187 560940

telex: 271148 SACENT I

VARIABILITY OF ACOUSTIC TRANSMISSIONS IN A SHALLOW WATER AREA,

by

16 Erik/Sevaldsen

11 1 MAY 81

13 52

This report has been prepared as part of Project 05.

APPROVED FOR DISTRIBUTION

B.W. LYTHALL
Director

Accession For	
NTIS GRA&I	<input checked="" type="checkbox"/>
DTIC TAB	<input type="checkbox"/>
Unannounced	<input type="checkbox"/>
Justification	
By	
Distribution/	
Availability Codes	
Avail and/or	
Dist	Special
A	

312 950

TABLE OF CONTENTS

	<u>Page</u>
ABSTRACT	1
INTRODUCTION	3
1 THEORY	7
2 PLANNING	11
3 EXPERIMENTS	15
4 PROCESSING	17
5 RESULTS	21
5.1 Relative Movements	21
5.2 Statistics	23
5.3 Spreading in Frequency and Time	25
5.4 Transmission Loss and Transmission-Loss Time Variations	34
6 DISCUSSION	41
CONCLUSIONS	49
ACKNOWLEDGEMENTS	51
REFERENCES	53

List of Figures

1. Effects of fluctuations in the medium on signals	4
2. Map on the experimental area, showing transmitter positions	12
3. Experimental situation	12
4. Signal characteristics	13
5. Matched filter outputs (envelope), 1. Ping group	18
6. Scattering functions (example)	19
7. Typical sound-speed profiles (summer and winter) measured in the area south of Elba	22
8. Relative movements	22
9. Statistics from one winter run	24
10. Statistics from one summer run	24
11. Spreading in frequency and delay, winter. Variable receiver depth, source depth: 15 m	26
12. Spreading in frequency and delay, winter. Variable source location, source on bottom receiver depth: 40 m and 54 m	28
13. Scattering functions with sidebands and wave spectra	29

TABLE OF CONTENTS (Cont'd)

	<u>Page</u>
14. Spreading in frequency and delay, winter. Variable source location, source depth: 45 m, receiver depth: 40 m	30
15. Spreading in frequency and delay, Winter. Variable source location, source depth: 15 m, receiver depth: P2 and P3 40 m, P1 and P5 40 m and 54 m	31
16. Spreading in frequency and delay, Summer. Variable source location	33
17. Transmission-loss time variations, Winter 78	35
18. Transmission-loss variations, Summer 78	36
19. Transmission-loss variability with position and receiver depth	38
20. Transmission-loss variability, summer and winter	39
21. Transmission-loss variability with source depth	39
22. Transmission loss: comparison between models and experiment	45
23. Ray tracings (GRASS), summer 77, positions 1 and 2	46
24. SNAP mode-energy vs arrival angle, Winter 78	47
25. SNAP mode-energy vs arrival angle, Summer 77	48

VARIABILITY OF ACOUSTIC TRANSMISSIONS IN A SHALLOW WATER AREA

by

Erik Sevaldsen

ABSTRACT

A series of experiments on the variability of acoustic transmissions in a shallow-water area is described. The variables considered have been time (short period and seasons), frequency of transmission (1 to 6 kHz), and space (location and depth of source, depth of receiver). The variability has been studied mainly in terms of transmission-loss fluctuations and spreading in frequency and delay of phase-coherent pulse signals. Short-period transmission-loss fluctuations have generally been found to be within ± 3 dB of the mean, with some few significant exceptions in summer. Delay spreading (3 dB) was found to be rather small, mostly near 5 ms, because there was usually only one strong arrival/arrival cluster. The measured frequency spreading can be classified in two groups, one showing very little spreading, Δf_c (0.05 to 0.1) Hz, the other being much more spread, $\Delta f > 1$ Hz. This is interpreted as the result of internal-wave action under the existing sound-propagation conditions, however, lack of environmental data prevents the provision of conclusive evidence for this explanation.

INTRODUCTION

When underwater acoustic signals propagate through the sea, the signals will be subject to changes due to the medium. By the medium we mean the water itself, its surface and bottom boundaries, and the sub-bottom sediments and rocks.

The medium through which the signals are being transmitted is partly random, partly deterministic.

It is random because the surface motion is more or less random and because we cannot know in detail the bottom composition and thus the effects of sound interacting with the bottom. In the water itself we find random temporal and spatial variations of the sound speed field. These variations occur over a very wide range of scales: from minutes to years and from centimetres to megametres. This variability is caused by internal waves in the water masses which, like surface waves, seem to exist at most places most of the time. Wherever there are density gradients, waves can propagate, and very often we find rather sharp temperature and density gradients in the ocean.

The medium must be considered partly deterministic because it also allows for coherent receptions under certain conditions (direct path, specular reflection, low density of inhomogeneities, etc.).

The effects of this partly random medium on underwater acoustic signals are observed most notably as amplitude and phase fluctuations and also as fluctuations in travel time. Thus a narrow-band signal will have its frequency band widened, and an impulsive signal will be stretched in time, (Fig. 1). There will be a loss in coherence of the signals with time and space, and the average level of the received signals will vary.

Table 1 lists important factors that cause signals to be spread in time and frequency.

In deep water the influence of one or both boundaries will generally be small. Here however, we are concerned with shallow waters, where, by definition, one is never far from the boundaries. The sea surface is almost always moving, causing doppler effects at all frequencies. The sub-bottom properties are of importance only for the lower frequencies, whereas the bottom slope and roughness also affect sound propagation at higher frequencies.

Sound-propagation conditions change with the time of the year, and the relative influence of the surface and the bottom thus changes accordingly. During the last decade considerable efforts have been made to explain and understand the mechanisms of these fluctuations in the ocean <1,2,3>. The works cited will provide a complete list of references.

In deep water far from boundaries, phase fluctuations can to a large extent be explained as being caused by internal waves. Amplitude fluctuations, however, cannot be accounted for completely by internal waves.

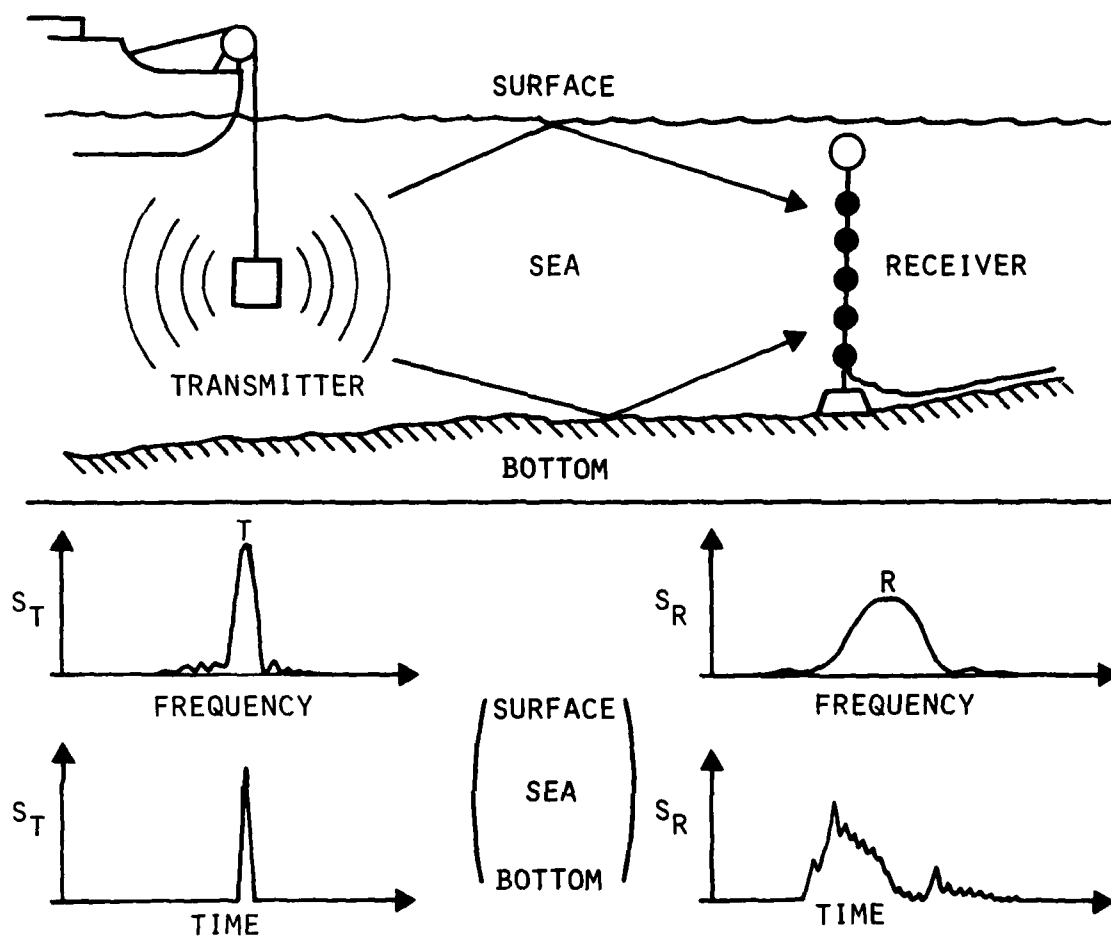


FIG. 1 EFFECTS OF FLUCTUATIONS IN THE MEDIUM ON SIGNALS

TABLE 1
IMPORTANT FACTORS CAUSING SPREADING IN FREQUENCY AND TIME

<u>FREQUENCY SPREADING</u>	
Caused by motion:	surface motion currents internal waves platform motion
<u>TIME SPREADING</u>	
Many paths between transmitter and receiver Different path lengths	
<u>FREQUENCY- AND TIME-SPREADING</u>	
Important factors:	
Range between transmitter and receiver Centre frequency of signal Time of the year	
In shallow water:	
Bottom vicinity Bottom type and slope Bottom sediment characteristics	

In shallow or coastal waters, internal waves cause fluctuations as in deep water, but the picture is confused because of the interaction with the boundaries and the effects of the moving surface. A deep-water internal-wave model is not applicable in most shallow-water situations.

All uses of underwater acoustic signals are affected by time variability in the medium: active and passive sonar, communications, and remote control. The effects on a system can be quite serious in terms of performance reduction. Loss in coherence, excessive variations in propagation loss, or large spreading can be caused, for instance, by wrongly selecting the frequency or depth of operation at a particular location and time of the year. Thus it is of considerable importance in any ASW context to understand the mechanisms involved and to be able to predict actual effects of the medium on signals propagating through the ocean. In particular, this applies to shallow or coastal waters.

1 THEORY

We have chosen to treat the shallow-water acoustic channel as a linear, time-varying filter <4 to 10>. There are of course other ways of analysing time variability of the medium, and the one chosen is not necessarily the best from all points of view. However, when the work started it was felt that our method would lead to the fastest results.

The linear, time-varying filter impulse response is

$$h(\tau, t)$$

We Fourier-transform this function with respect to the time variable to find the channel-spreading function

$$s(\tau, \phi) = F\{h(\tau, t)\}. \quad (\text{Eq. 1})$$

This function gives the spectrum of the time variations of the impulse response.

In general, the detailed time behaviour of the filter functions will not be known. The impulse response of $h(\tau, t)$ may be considered as a sum of a large number of elementary impulse responses associated with the various paths and physical effects that distort a signal along a path.

There are two types of elementary contribution to the global impulse response.

- a) Deterministic: multipath effects, reflections from flat boundaries.
- b) Random: caused by scattering from inhomogeneities in the water masses and from the rough boundaries.

The information content in a signal that has passed through a deterministic channel can, in principle, be restored. A random channel must be described in a statistical way, and the random effects cannot be compensated for in the receiver.

A random, time-varying channel can be described by the autocorrelation functions of its system functions. Two of them are:

$$R_h = R_h(\tau, \tau', t, t') = \overline{h(\tau, t)h^*(\tau', t')} \quad (\text{Eq. 2})$$

$$R_s = R_s(\tau, \tau', \phi, \phi') = \overline{s(\tau, \phi)s^*(\tau', \phi')} \quad (\text{Eq. 3})$$

(impulse response and spreading function, see also <6> and <7> for more about system functions).

These four-dimensional correlation functions are inconvenient to use. Introducing some restrictive assumptions on the underlying random processes reduces the number of dimensions to two:

- a) Wide-sense stationarity in time, which is equivalent to uncorrelated scattering in frequency. R_h depends only on time difference, $R_s = 0$ for $\phi' \neq \phi$.

- b) Uncorrelated scattering (in time), equivalent to wide-sense stationarity in frequency. $R_h = 0$ for $\tau \neq \tau'$.

This results in

$$R_h = \overline{h(\tau, t)h^*(\tau', t') \cdot \delta(\tau - \tau')},$$

$$R_h = R_h(\tau, \Delta t) \cdot \delta(\tau - \tau'), \quad (\text{Eq. 4})$$

$$R_s = \overline{s(\tau, \phi)s^*(\tau', \phi') \cdot \delta(\tau - \tau') \cdot \delta(\phi - \phi')},$$

$$R_s = \overline{|s(\tau, \phi)|^2} \cdot \delta(\tau - \tau') \cdot \delta(\phi - \phi'),$$

$$R_s = R_s(\tau, \phi) \cdot \delta(\tau - \tau') \cdot \delta(\phi - \phi'). \quad (\text{Eq. 5})$$

The function $R_s(\tau, \phi)$ is called the scattering function. It has received special attention in radar and sonar because under certain conditions it determines the spreading in frequency and time of a radar or sonar signal. One of these conditions is that the transmitted signal has a narrow ambiguity function.

The ambiguity function of a signal $x(t)$ is derived from the correlation function of the signal with a delayed and frequency-shifted version of itself:

$$X(\tau, \phi) = \int_{-\infty}^{\infty} x(t)x^*(t - \tau)e^{j2\pi\phi t} dt. \quad (\text{Eq. 6})$$

The squared quantity $|X(\tau, \phi)|^2$ is defined as the range/doppler ambiguity function of the signal. Under ideal conditions of the medium the signal ambiguity function determines the resolution in time and frequency of an echo-locating system, provided the target is a point target. In a random medium the resolution in time and doppler of the same system will be expressed by an ambiguity function

$$P(\tau, \phi) = \iint_{-\infty}^{\infty} |X(\tau - u, \phi - v)|^2 R_s(u, v) du dv. \quad (\text{Eq. 7})$$

This function can be interpreted as the combined ambiguity function of the signal and the medium obtained by convolving the signal ambiguity function with the scattering function of the medium. From Eq. 7 we see that if the scattering function is wide compared with the signal ambiguity function, the resolution in delay and doppler is completely determined by the scattering function:

$$P(\tau, \phi) = R_s(\tau, \phi) \cdot \iint_{-\infty}^{\infty} |X(\tau - u, \phi - v)|^2 du dv$$

$$= R_s(\tau, \phi). \quad (\text{Eq. 8})$$

Under the assumptions of wide-sense stationarity and uncorrelated scattering (WSSUS) an estimate of the scattering function of the medium can

be obtained by simply averaging the spreading functions magnitude squared.

$$R_s(\tau, \phi) = \overline{|s(\tau, \phi)|^2} \quad (\text{Eq. 9})$$

To compute $s(\tau, \phi)$, the spreading function, we need estimates of the channel impulse response. The obvious solution would be to transmit a very short pulse. This signal has a small energy content, and detection range would be short.

To increase pulse energy and range coverage, we can use a coded pulse with bandwidth duration product $BT \gg 1$. This signal has to be matched filtered on the output of the time-varying filter and this MF output is taken as the estimate of the channel impulse response. A train of phase coherent (equal) pulses will provide a sequence of impulse response estimates all referenced to the same phase or delay. To compute $s(\tau, \phi)$, from $h(\tau, t)$ we need a certain number of pings or impulse responses to form the matrix in delay and time over which we do the Fourier transform.

The final resolution in frequency is determined by the dimension in time of the matrix. In delay, the resolution is determined by the bandwidth of the individual pulses.

Filter time variability may include both deterministic and random components. A filter of this type is said to be partially coherent $\langle 7 \rangle$, and it is modelled by two filter blocks in parallel, one purely deterministic and one completely incoherent. The deterministic part, which may or may not include DIRAC pulses, represents the mean value or first-order statistics of the random processes characterizing the channel. The random part of the filter represents the deviations around the mean, i.e. the second-order statistics of the process. However, the distinction between the random and deterministic processes may not always be obvious.

The existence of a scattering function requires that the medium processes should be wide-sense stationary in both time and frequency (and space). None of these conditions is strictly fulfilled:

- a) The channel characteristics vary with weather conditions, time of the year, day and night, and from hour to hour (or minute).
- b) The combined effect of the channel seems to be strongly frequency dependent.
- c) Propagation conditions differ with position of both source and receiver in all three dimensions.

However, one can easily accept the concept of a scattering function being valid at a certain location and for a limited frequency band and period of time. This weaker condition of local stationarity may still be a useful concept provided that the time, frequency, and space windows are not too small. And the scattering function itself should not vary too much from one window to another.

2 PLANNING

We wanted experimentally to investigate characteristics of the fluctuating shallow-water medium and to study the effects on underwater acoustic transmissions. Specifically we wanted to measure the spreading effect of the medium in frequency and time on one-way transmitted signals. Also time variations of transmission loss should be included. The idea was to make the measurements with space, time, and frequency as variables. Limitations in experimental time, equipment, and support determined to a large extent the set-up. In particular it was essential to use existing equipment.

The area south of Elba was chosen for the experiments because of SACLANTCEN's installations on the Formiche di Grosseto islands, which provided a fixed receiving point for transmissions (Fig. 2). Figure 3 shows the experimental situation. Depending on the frequency used, the results would be more or less area dependent. However, the available transducers limited the frequency range downwards to about 1 kHz. This means that only the upper few metres of the bottom sediment had any influence on the results.

The frequency band covered (1 to 6 kHz) is high in a passive sonar sense and low for communications. But it is wide, and the results should tell us something about trends with frequency.

Variability in space was included by

- ☐ transmitting from five pre-selected positions
- ☐ transmitting from three different depths
- ☐ receiving on a vertical hydrophone array

Time variability was taken care of by doing three series of measurements during the year.

Processing of data should be through the spreading functions and scattering functions, which will give us the combined spreading effect of the channel. Several types of signals should be used: long-CW, PRN-modulated signals and linear-FM sweeps. For the spreading function computations we decided to use phase-coherent linear FM sweeps as the main signal. Signal characteristics are summarized in Fig. 4, which also shows the transmission channel with input and output signals.

It should be noticed that up to six signals with different centre frequencies, but otherwise identical, were added and simultaneously transmitted. Phase coherence implies that all pulses transmitted have the same phase (and amplitude) at all delays, i.e. they are identical. The way we decided to analyse our signals works only if the channel is underspread, i.e. the product of frequency spread and time spread is less than one ($F_s \cdot T_s < 1$).

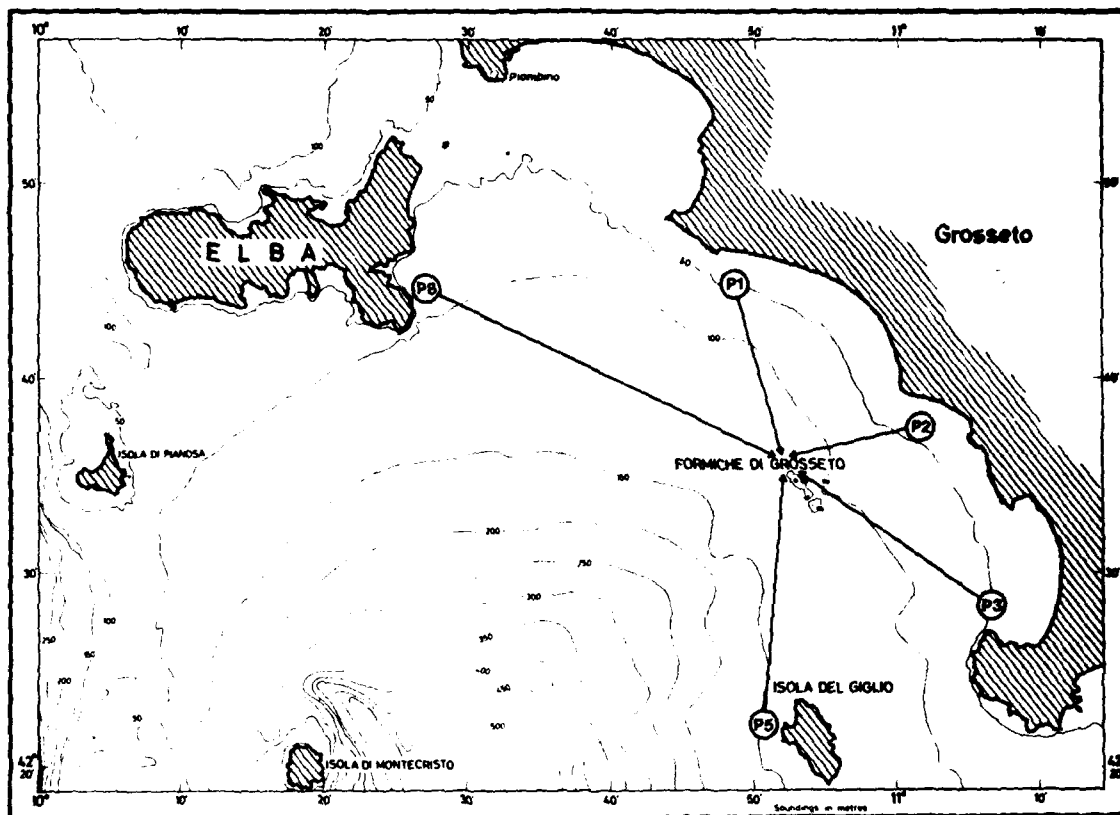
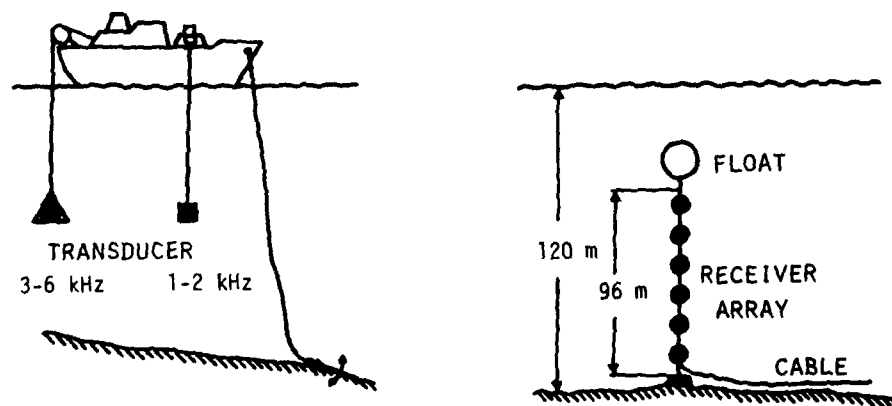


FIG. 2 MAP OF THE EXPERIMENTAL AREA, SHOWING TRANSMITTER POSITIONS



POSITION	RANGE	DEPTH	
		SUMMER	WINTER
1	16 300 m	67 m	68 m
2	12 800 m	58 m	56 m
3	22 100 m	60 m	54 m
5	25 300 m	70 m	124 m
8	38 500 m	80 m	65 m

FIG. 3 EXPERIMENTAL SITUATION

BASIC SIGNAL:

COHERENT PULSE TRAIN
OF LINEAR FM PULSES

PULSE LENGTH	125 s
PULSE BANDWIDTH	500 Hz
PULSE REPETITION PERIOD	1.0 s
CENTRE FREQUENCIES	1,2,3,4,5,6 kHz

TRANSMITTED SIGNAL:

SUM OF ALL 6 BASIC SIGNALS
OR 4 OF THEM
OR 2 OF THEM

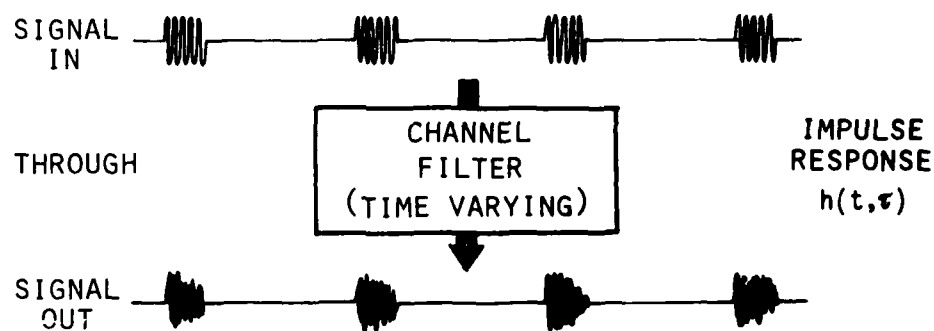


FIG. 4 SIGNAL CHARACTERISTICS

3 EXPERIMENTS

We made three series of experiments: in spring, summer, and winter. During each experiment the ship anchored at one of the selected positions (Figs. 2 and 3 sketch the situation). When the ship had attained a stable position the transducers were lowered to the first depth and transmission started. Two separate transducers had to be simultaneously used to cover the 1 to 6 kHz frequency band. Three different depths were chosen:

- ☐ in the mixed layer, 10 m or 15 m;
- ☐ below the thermocline, usually 45 m;
- ☐ on the bottom.

Unfortunately the transducer used for the 1 and 2 kHz signals could not be placed on the bottom.

It was found that a pulse-repetition frequency of 1 Hz did not cause signals to overlap in time at the receiving end. This means that the channel is underspread provided that the 1 Hz medium sampling rate is high enough.

The receiving array was a vertical array moored near the Formiche di Grosseto islands, for which two different arrays were used. In spring and summer we used a short array covering 14 m of water depth between 40 and 54 m. The winter array covered virtually the whole water column from 26 to 116 m (Fig. 3). Water depth at the receiving end was 120 m. Eight hydrophone signals were amplified, filtered, and stored on analogue magnetic tape. The transmissions lasted approximately 30 minutes at each transducer depth and for each signal type, which was considered a reasonable period over which to do the processing. The main signal, consisting of linear FM pulses, was transmitted at all positions and transducer depths. In some cases this signal was supplemented with transmissions of long-CW and PRN-modulated signals. Measurements were continued with the transmitters at the second depth and on the bottom. The ship then moved to the next position. Sound-speed profiles were taken at both ends of the transmission paths and in summer also at a third position along the paths.

4 PROCESSING

Analysis of the recorded hydrophone signals had to be done off-line in the laboratory. To arrive at the spreading effect of the medium we needed estimates of the impulse response of the transmission channel. For this purpose we used the received signals matched-filtered with the transmitted signal, each frequency band being treated separately. 128 consecutive pulses, denoted a ping group, were used to form a matrix of matched filter outputs or channel impulse responses.

Figure 5 shows the envelope of one matrix of matched-filter outputs (a ping group) from one particular run. The variations of these impulse responses with time were Fourier-transformed to give the channel-spreading function for that particular set of pulses. Note that in the computations we used the matched-filter output signal itself and not the envelope.

Sometimes, when the transducers were suspended from the ship, ship drifting showed up in the results as a changing delay. This is clearly a non-stationary trend and had to be removed, which was done by aligning the matched-filter outputs following an averaged delay curve to ensure that fluctuations were not taken out.

From each ping group we computed a spreading function. The spreading function magnitude squared (SFMS) is a sample function of the so-called scattering function (SF). Averaging over all SFMSs gives us an estimate of the scattering function.

To determine if the SFMSs could be averaged to yield better estimates of the scattering function we had to check the stationarity of process. The statistical tests were done on the aligned matched filter outputs before computing the spreading functions.

We checked the independence of the process with a runs test, and the stationarity (provided independence) with a Kolmogorov-Smirnov test. Each frequency band was treated separately. The tests and test statistics are described in <11 to 14>.

The one-sample runs test was applied to the individual ping groups. For each delay value (Fig. 5) we computed the number of runs over the ping group (time). The number of runs for a particular delay is defined as the number of sign changes plus one.

We also computed the mean value and standard deviation of the matched-filter output samples over time for each delay value, i.e. over the same samples used in the runs test. However, the calculations were here made cumulative over the ping groups. If the data fail the independence test, a comparison of the mean and standard deviation gives some indications as to whether the data can be considered incoherent or not, i.e. if the assumption of uncorrelated scattering is justified. Independence of the process implies incoherence, but not vice versa.

The Kolmogorov-Smirnov two-sample stationarity test was applied to the same data. It compares the experimental cumulative amplitude distribution functions of two sample sets. Changes in the underlying processes show up as changes in the probability density and distribution functions, and the

test is sensitive to these changes. We computed the experimental cumulative amplitude distribution function for all pings in a ping group, and this distribution function was then compared with the cumulative distribution function over all previous ping groups.

The usefulness of the scattering function estimates rather than the individual SFMSs as a basis for extracting spreading information is determined by the outcome of the statistical tests.

An example showing a set of scattering functions is shown in Fig. 6. The situation is the same as the one depicted in Fig. 5, which shows the first ping-group matrix used in forming the scattering function (Fig. 6). For the processing we used the ITSA (Interactive Time Series Analysis) system developed at SACLANTCEN.

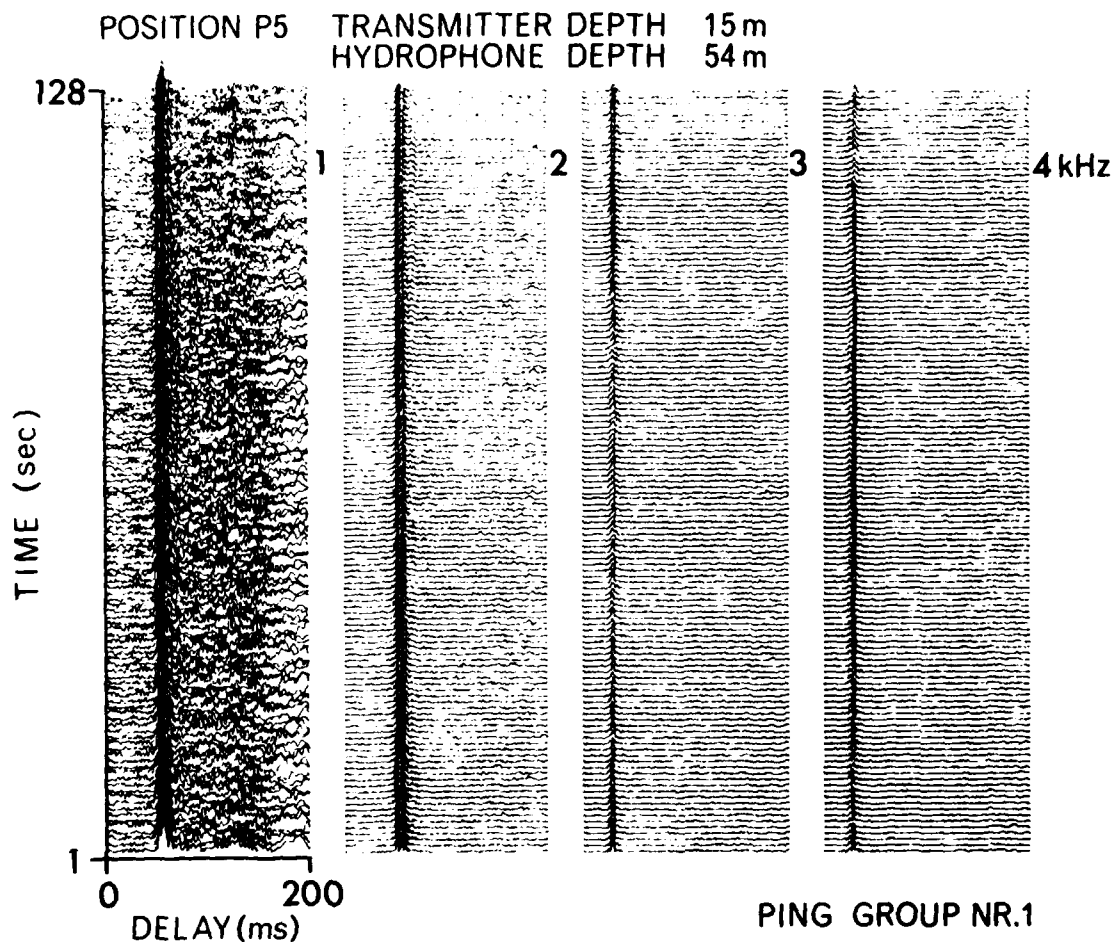


FIG. 5 MATCHED FILTER OUTPUTS (envelope), 1. PING GROUP

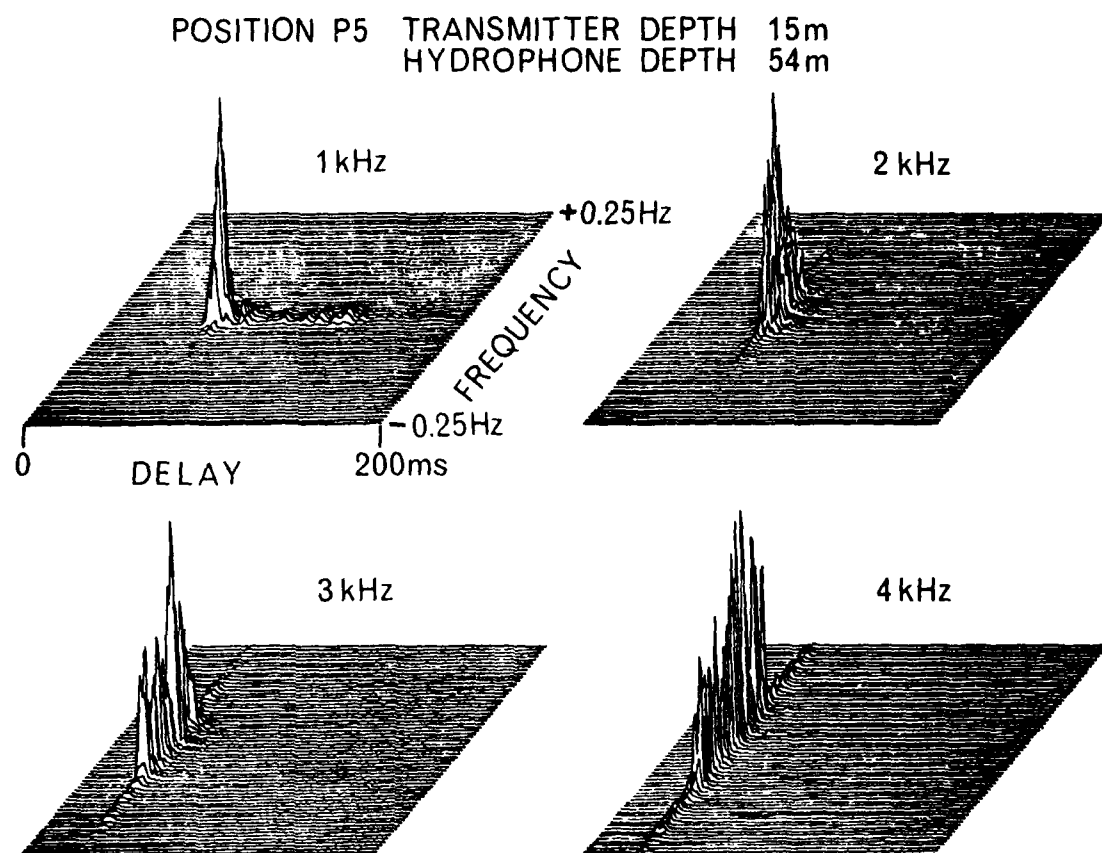


FIG. 6 SCATTERING FUNCTIONS (example)

5 RESULTS

Data from the spring (PILOT) experiment were of little value because of an unstable signal-generator clock. We are left with the summer and winter data, which exhibit the typical or stable sound-propagation conditions. Spring and autumn conditions in the Mediterranean always represent transition periods in which conditions change from one stable type to the other. Figure 7 shows typical sound-speed profiles from summer and winter measured in the area south of Elba.

5.1 Relative Movements

Relative movements between source and receiver cause doppler shift and delay variations in the received signals. Our receiving array was a moored vertical string of hydrophones, which we consider fixed. Relative movements come from using transducers suspended from the anchored ship. Delay variations represent unstationary trends that must be removed. The changing delay shows up not only as slow variations in arrival time but also as phase changes in the received signals. We have found that the doppler shifts are generally small, but any doppler will also change the signal phase by changing the frequency. We removed the arrival-time trend by aligning the matched-filter outputs following an averaged delay curve. In this way fluctuations in delay were not removed. Neither the phase changes caused by the delay variations nor the doppler effect were however compensated for. They show up in the results as shifts in frequency of the spreading functions. The shift curve seems to follow the delay curve with some phase shift.

If the shifts are too great, the use of a scattering function is not justified. This is because its width in frequency is determined not by effects in the medium but by shifts caused by the changing delay.

Figure 8 shows a comparison between two situations, one with the transducer on the bottom, i.e. no delay variations, and another with a lot of movements. The left parts of the figure show projections of spreading functions magnitude squared (SFMS) on the frequency axis while the right parts show projections of the same functions on the delay axis. The uppermost curves in both sets show projections of the scattering functions, i.e. the average of all 14 SFMSs below. We see from the bottom results presented (Fig. 8a) that also here there are small shifts in frequency between the spreading function projections. These shifts have been caused by fluctuations in the medium. The width in frequency of the scattering function is interpreted as the total bandwidth necessary to receive a narrow-band signal having passed through the time-varying medium. The individual spreading function projections generally show less width. Tests indicate that it is not the analogue tape recorder that is causing the small shifts.

The example with delay variations (Fig. 8b) clearly shows that the scattering function is much less useful. The individual spreading functions are much narrower in frequency than the scattering function. Variability of the medium has been lost in the movements. In cases like this we will disregard the scattering function.

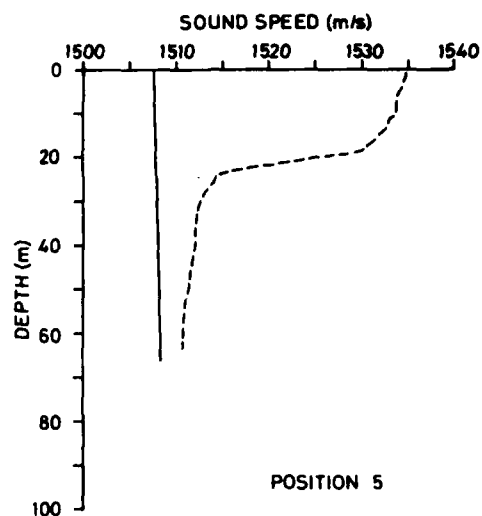


FIG. 7 TYPICAL SOUND-SPEED PROFILES (summer and winter) MEASURED IN THE AREA SOUTH OF ELBA

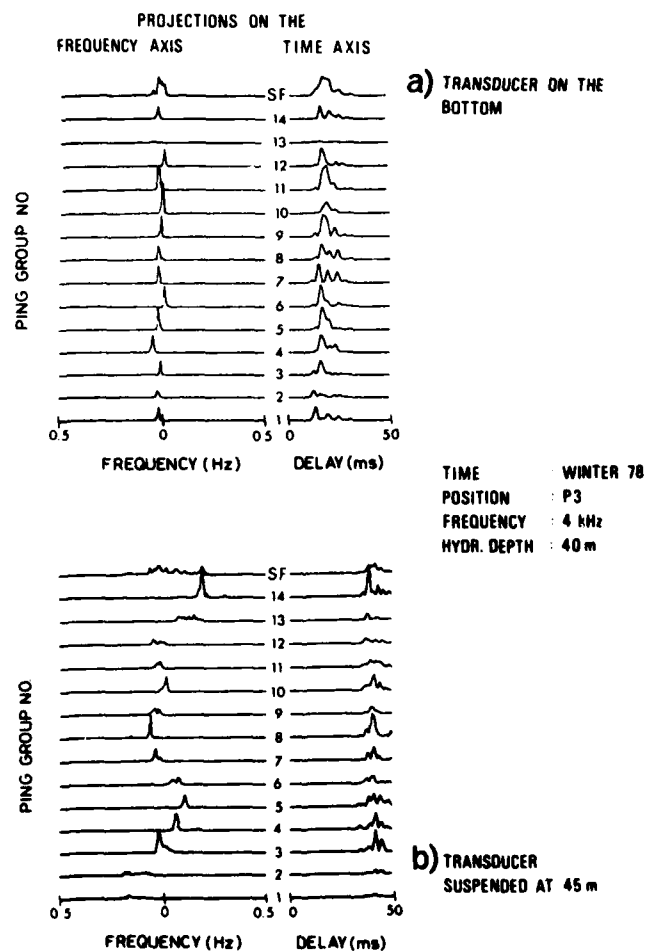


FIG. 8 RELATIVE MOVEMENTS

Comparing the widths in frequency of the individual spreading functions in the two examples of Fig. 8 we find that the widths with the suspended source are somewhat larger than with the source on the bottom.

We do not believe that the differences observed are due to different source depths. It is much more likely that the increased frequency spreading is caused by movements of the source, in radial and transversal direction. However, the differences in spreading between the two cases shown are rather small, which indicates that the spreading effect of source movements is quite small.

The spreading function information will be presented as a weighted average of the widths in frequency and delay over the ping groups. The weight will be the (relative) amplitude of the individual spreading functions. We do it this way because the amplitudes are smallest where the frequency spreading caused by movements is the largest (see Fig. 8b). Our method thus reduces the influence of the effect of movements on the results.

5.2 Statistics

Statistics of the underlying random processes have been checked in two ways: by a one-sample runs test for independence and by a two-sample Kolmogorov-Smirnov test for stationarity. We also computed mean values and standard deviation over time as a function of delay for the matched filter outputs, a kind of coherence check on the data. The significance levels were chosen to be 5%. For the process to be stationary the data must pass both tests since a process is stationary, following the K-S test only if it is also independent. If the process is independent the conditions of uncorrelated scattering is also met.

Summarizing the results of the statistical tests we see that the data almost failed the independence test whereas they very often passed the K-S test. For winter data the runs test usually showed the number of runs to be too small, especially at lower frequencies.

Testing summer data we sometimes found that the number of runs was too large. The first results can be interpreted as indicating the presence of low-frequency (deterministic) component(s) that have been high-frequency sampled (oversampled) in time. The summer results indicate that there may be components present - deterministic or not - that have been undersampled.

Figures 9 and 10 show results, from winter and summer respectively, for:

- a) independence test,
- b) coherence check
- c) Kolmogorov-Smirnov stationarity test.

We have found that in most cases the process is not stationary. This in fact should exclude the use of scattering functions. However, we still think that it may be useful to compute and present them at least as a comparison with the SMFSs for the following reasons:

- The unstationarity seems to be caused by the presence of deterministic components in the received signals.

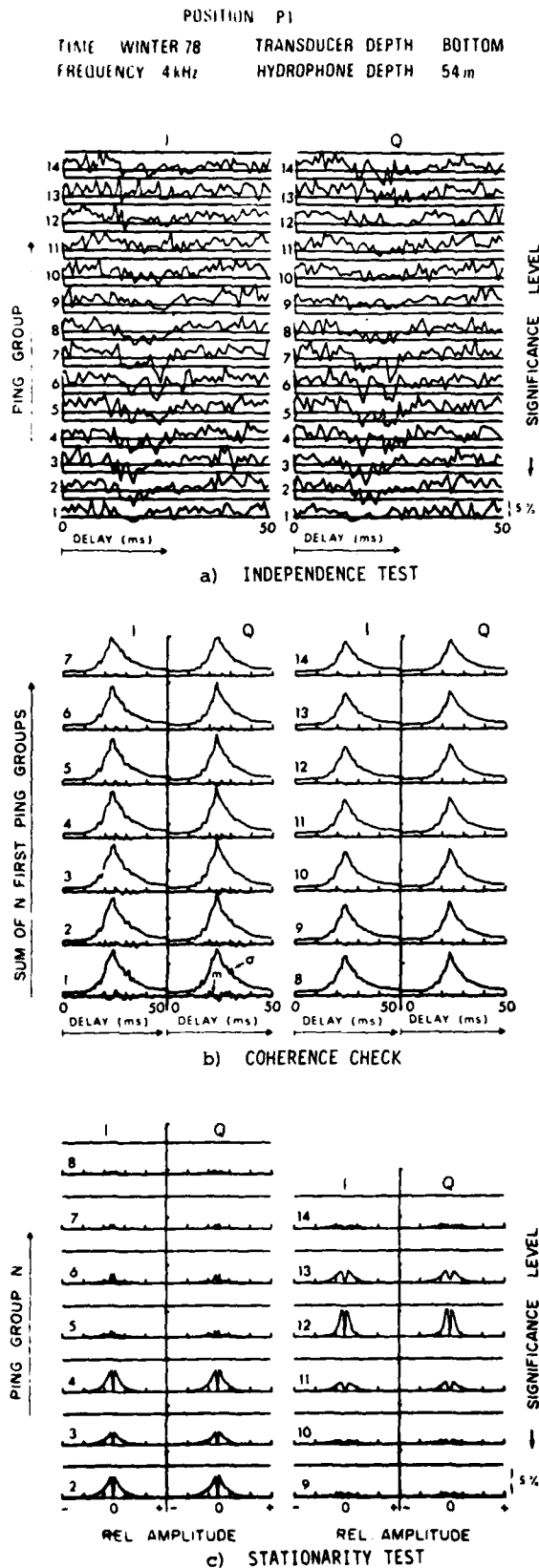


FIG. 9
STATISTICS FROM ONE WINTER RUN

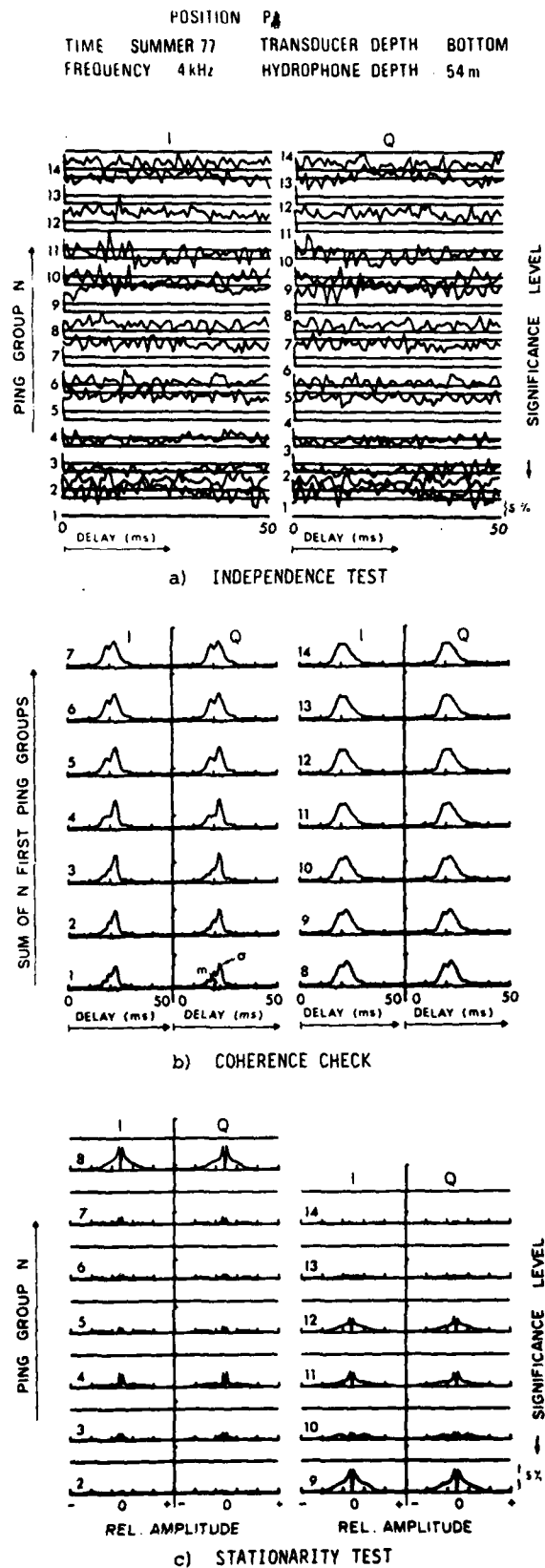


FIG. 10
STATISTICS FROM ONE SUMMER RUN

- The coherence check indicates that the process may still allow for uncorrelated scattering in many cases.

We also observe that in most cases the data pass the Kolmogorov-Smirnov stationarity test at the 5% significance level chosen. It is, however, equally clear that from time to time the processes change a lot from one ping group (matrix) to the next (see Figs. 9c and 10c).

Comparing the runs tests (Figs. 9a and 10a) we see that there is a lot more variability in summer than in winter. The Kolmogorov-Smirnov test results shown in Figs. 9c and 10c on the other hand do not differ significantly from summer to winter. This indicates that the processes involved tend to be locally stationary over approximately the same time periods, both in summer and winter. The Kolmogorov-Smirnov tests are sensitive to changes in amplitude distribution of the received pulses. In our case it means changes in level and time length of the received signals caused by changes in the mode/multipath structure. In a runs test noiselike signals tend to have a medium number of runs. Strong low-frequency components lead to few runs, while the presence of strong high-frequency components (signals may be undersampled) lead to many. A runs test measures phase changes between the received pulses and is sensitive to changes in the frequency content (spectrum) of the time variations of the medium. Fluctuations detected by the runs tests are associated with changes in width and/or position in frequency of the corresponding spreading functions.

From the case displayed in Fig. 10 we find that the underlying processes have been undersampled for some ping groups (spreading functions). However, not all summer data have been undersampled. We also find cases where the frequency spreading is small, as in most winter results.

We have observed that changes in the spectrum of time variations of the medium do not seem to be associated with corresponding changes in amplitude distribution and vice versa. It seems that the mechanisms causing frequency spreading are different from those causing delay spreading and variations in level (or transmission loss).

5.3 Spreading in Frequency and Time

Two types of results will be presented. First we present the weighted average of the total 3 dB width of the spreading functions. This can be looked upon as a short-term (2 min) value of the spreading effect of the medium. The averaging is done over the number of ping groups, usually 14. We also present the widths in frequency and delay of the scattering functions. These values should be seen as the total spreading effect of the medium, which comprises both the spreading over the individual ping groups and the shifts between ping groups, which also are caused by the medium. However, if the SF frequency spreading is significantly greater than that found from the SFMSs we will check whether relative movements cause this difference.

We start with winter results. Figure 11 displays the effects of varying the receiver depth at position P5, shallow transducer. Spreading taken from the scattering functions (a) and from the weighted averages of spreading functions magnitude squared (b) are compared. Receiver depths

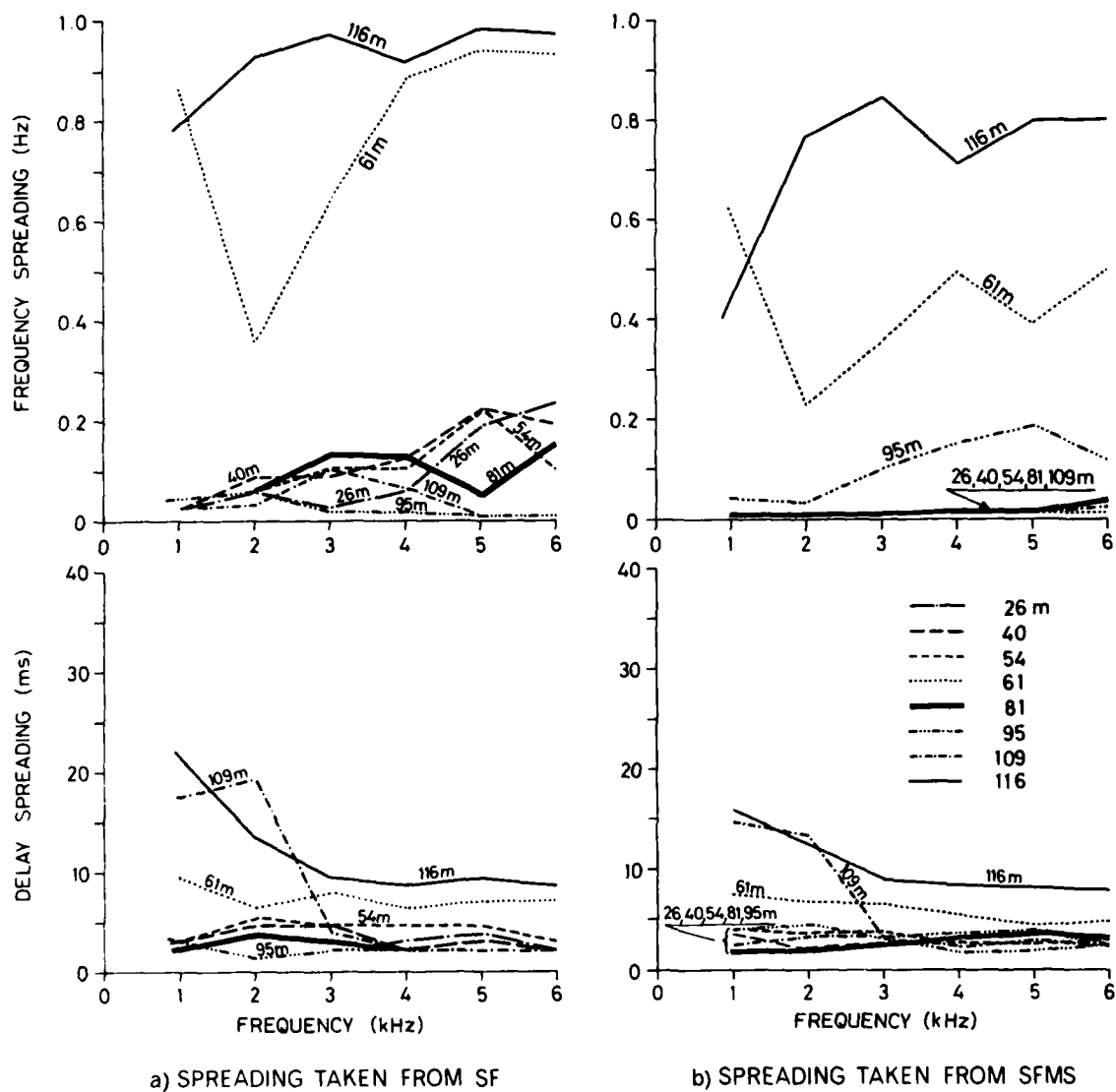


FIG. 11 SPREADING IN FREQUENCY AND DELAY, WINTER.
VARIABLE RECEIVER DEPTH, SOURCE DEPTH: 15 m

116 m and 61 m show much more spreading in frequency than do signals from other hydrophone depths. Actually the processes due to the medium have been partly undersampled here. The differences seen between a) and b) for the signals with low spreading are thought to be significant, i.e. the shifts between individual spreading functions that cause the SF to be wider than the SFMS reflect real processes due to the medium and not movements of the source. The total frequency-spreading effect of the medium lies from 0.1 Hz to 0.2 Hz for these signals, whereas spreading that excludes medium-induced frequency shifts is some 10% of this.

The signals received at 95 m are different from the others. Width in frequency of the SFMSs is greater than the SF width, which is unusual. It seems that the underlying processes have changed during the run. Most of the received signals must be classified as incoherent, like the 116 m and 61 m signals. But for that part of the run covering approximately five spreading functions (9 to 13), highly coherent signals are received. When the signals change, the signal delay changes also. It seems that we are observing a change in the mode or path structure where two arrival types are replacing each other. A weighted average of the resulting SFMSs comes out as something in between, as seen in Fig. 11b.

It is clear that the signals received at 116 m and 61 m, and partly at 95 m, are very much different from the rest in terms of frequency spreading or coherence in time. Also, delay spreading is greater for the two first-mentioned hydrophone signals and, to some degree, for the one at 109 m: around 10 ms, compared with less than 5 ms for the rest of the hydrophones. Signals from these other hydrophones seem to be quite equal in terms of spreading and indicate that one can average. Most of our data are signals from 40 m and 54 m depths. The results presented below have been averaged over these two hydrophone depths whenever possible.

Figure 12 shows winter results averaged over receiver depths 40 m and 54 m, with the transducer on the bottom. Again a) and b) compare spreading taken from SF and SFMS respectively. We see that a) gives little more spreading than b), with the exception of position P2. The P2 signal is much more spread in frequency than the other signals and has essentially been undersampled. The spreading in frequency of signals from positions P3 and P5 is very small, close to the resolution of the system.

In Fig. 12 the data from position P1 are different in that they show a marked increase in spreading as the centre frequency of transmission increases. It turns out that the P1 spreading functions have side-bands. During the P1 runs described here the surface-wave spectrum was rather peaked. The observed side-bands are shifted from the central spreading function peak by this main wave frequency. The wave spectrum and four scattering functions from this run are shown in Fig. 13. The width of the central peak is small, as with P3 and P5. Delay spreading is low in all cases, around 5 ms, and nearly constant over the frequency band.

Additional winter results are presented in Figs. 14 and 15 for transducers suspended at 45 m and 15 m respectively. From Fig. 14 we see that some of the results are not very different from the bottom cases at positions P3 and P5: delay spreading near 5 ms and small spreading in frequency. The SF frequency spreading (Fig. 14a) from positions P2 and P3 must, however, be disregarded because of source movements. The shallow-transducer case (Fig. 15) shows some increase in frequency spreading relative to the deep-

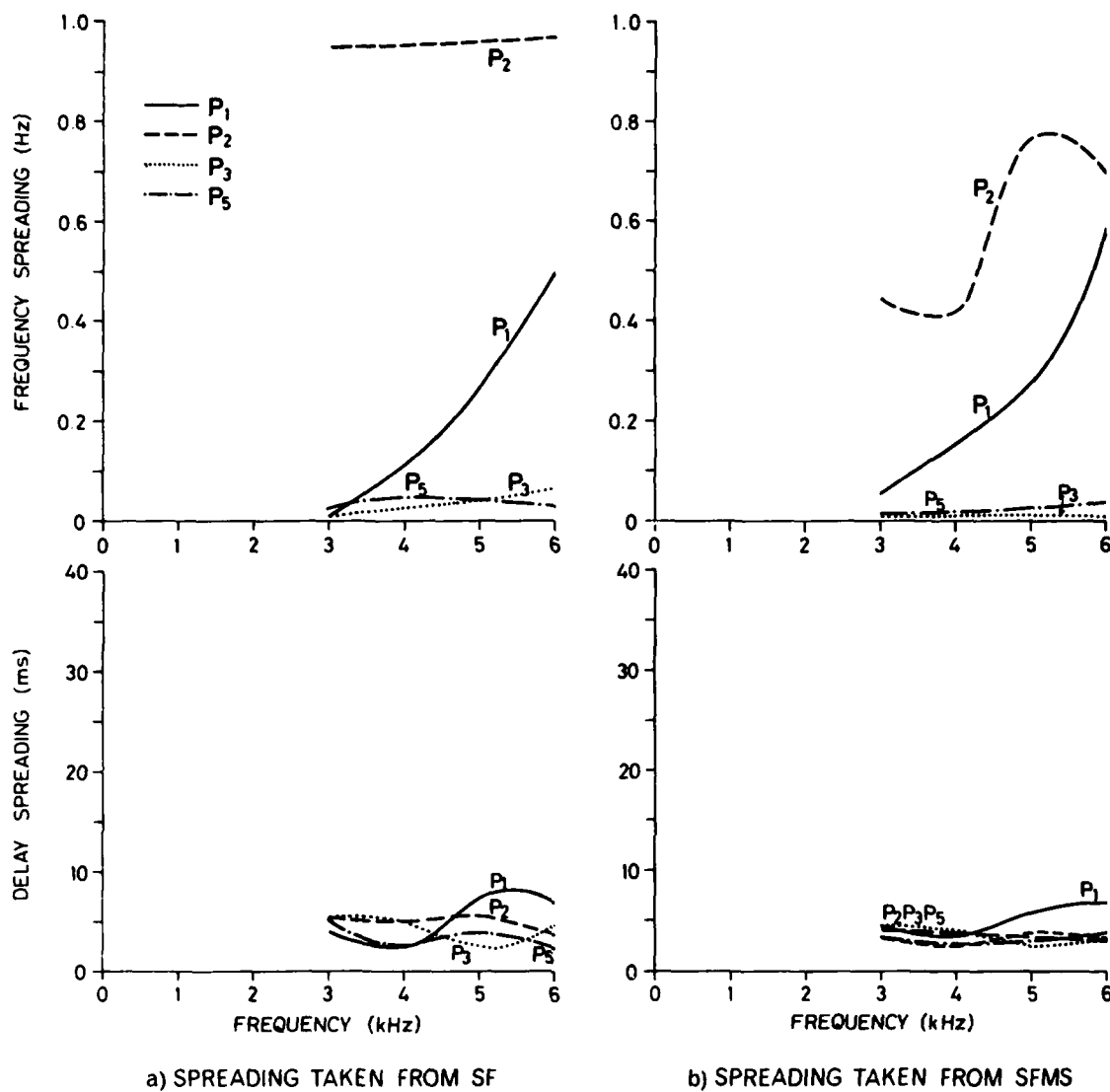


FIG. 12 SPREADING IN FREQUENCY AND DELAY, WINTER.
 VARIABLE SOURCE LOCATION, SOURCE ON BOTTOM
 RECEIVER DEPTH: 40 m and 54 m (averaged results)

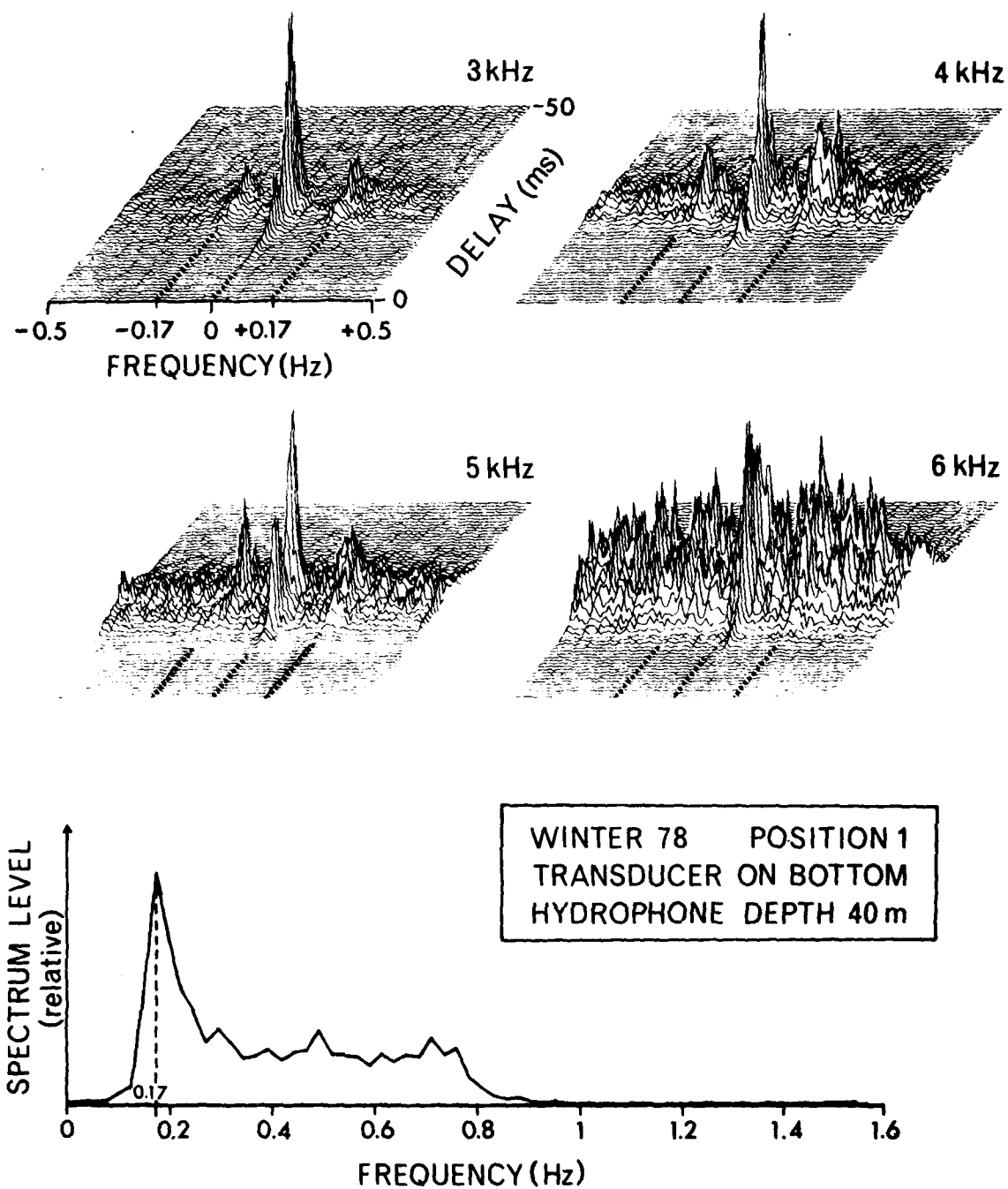


FIG. 13 SCATTERING FUNCTIONS WITH SIDEBANDS AND WAVE SPECTRA

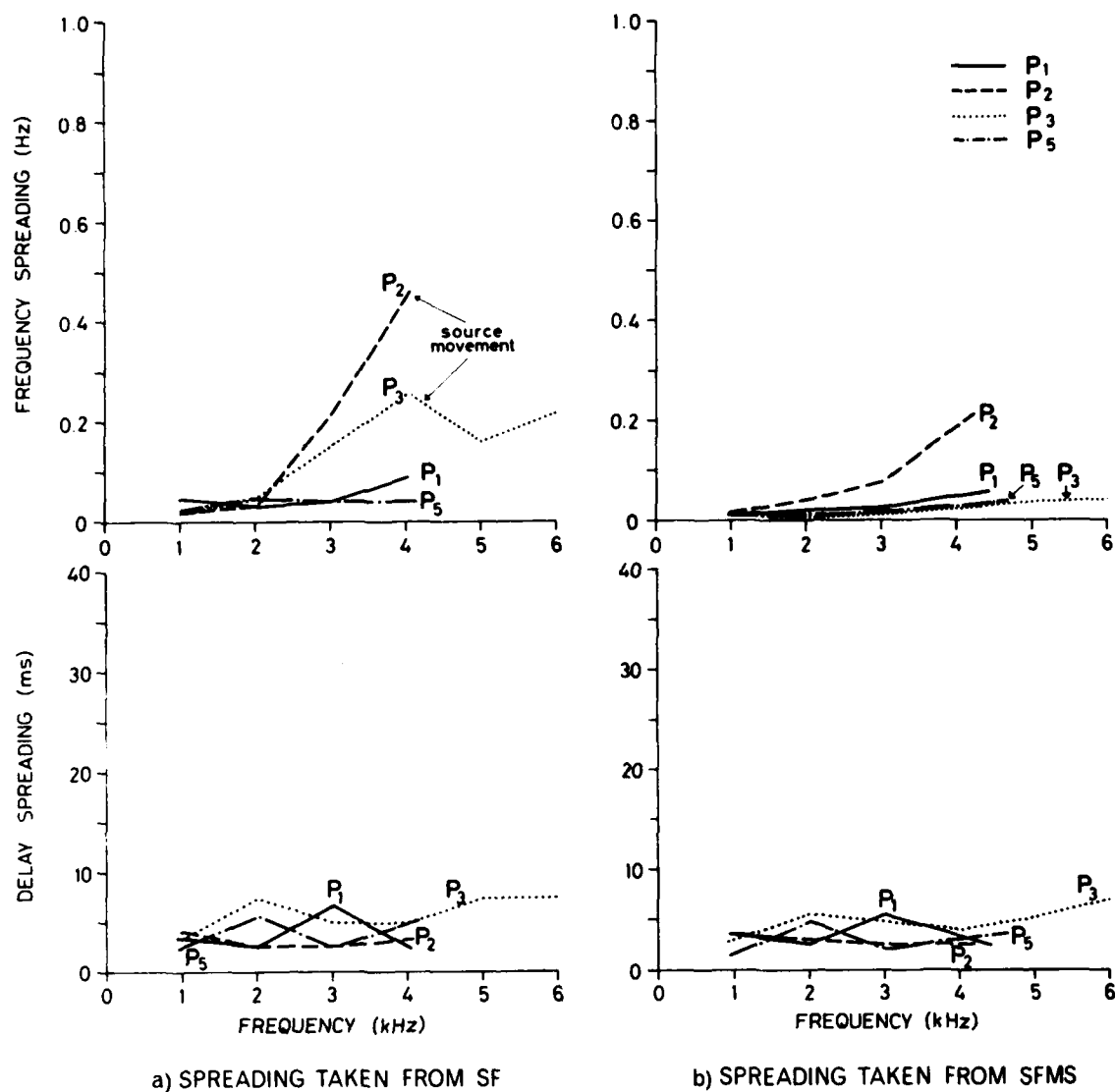


FIG. 14 SPREADING IN FREQUENCY AND DELAY, WINTER.
 VARIABLE SOURCE LOCATION, SOURCE DEPTH: 45 m,
 RECEIVER DEPTH: 40 m

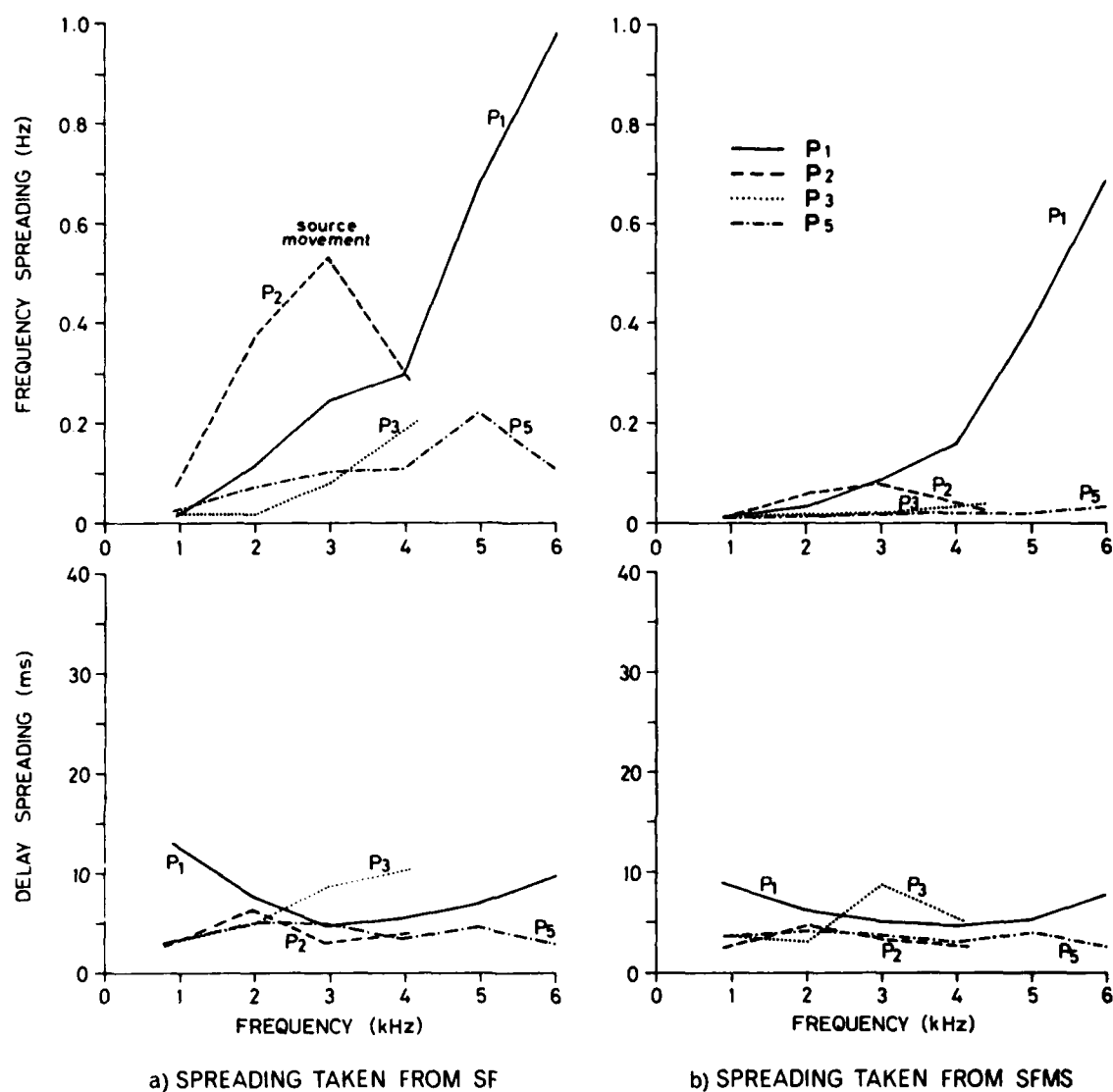


FIG. 15 SPREADING IN FREQUENCY AND DELAY, WINTER.
 VARIABLE SOURCE LOCATION, SOURCE DEPTH: 15 m,
 RECEIVER DEPTH: P_2 and P_3 40 m, P_1 and P_5 40 m
 and 54 m (averaged results)

suspended case. Also here we reject the SF frequency spreading from position P2 because of movements. All SF curves to be disregarded because of movements are marked. The other SF curves may reflect true medium effects except the 5 and 6 kHz cases at P1, which have been undersampled. However, we observe rather big differences between the SF curves (a) and the SFMS curves (b). It is possible that these differences are due to process unstationarity, as mentioned above.

The P1 frequency spreading is seen to increase with frequency (Fig. 15). This is probably caused by the rough surface, as in the P1 case with the source on the bottom. The surface waves had a rather peaked spectrum. No clear sidebands are observed, however, because this time we worked with a suspended source.

Widening in frequency caused by interaction with the surface is also visible in the P1, deep transducer results. The effects are seen to be weaker here than with the shallow transducer.

Spreading functions from position P2 also exhibit some increased width in frequency. Actually, because of undersampling of the spreading functions (large shifts caused by source movements and medium effects) the P2 curve, shallow transducer, does not increase so much as it otherwise would have done towards higher frequencies. The increased width is believed to be caused by a combination of source movements and surface roughness. We cannot compare this with the bottom run since it is one of our group 2 (undersampled) runs. Comparing with Fig. 8b we find that the observed widening in frequency of the spreading functions is considerably greater at P2 than at P3. We conclude that surface roughness in this case also contributed to the overall frequency spreading even though the wave spectrum was found to be flat. In the two results at P1 and P2 where we observed this (rather weak) surface influence the direction of transmission was more or less downwind. At positions P3 and P5 direction of transmission was near crosswind. Sea state was comparable at P3 and lower at P5. We observed no widening in frequency of the spreading functions at P3 and P5. This indicates that downwind (or upwind) transmissions may cause more frequency spreading than crosswind transmissions.

What we have said here applies to winter data only. In summer sound interaction with the surface is much weaker, and it is not likely that this surface influence will be seen.

Summer results are displayed in Fig. 16. Only part of the summer data have been analysed. As before, a) and b) represent SF (scattering function) and SFMS (spreading function magnitude squared, weighted average) results respectively. Three bottom runs (P1, P2 and P3) and two runs with suspended transducers (P5) are shown. All these runs except the one with the shallow suspended transducers show large frequency spreading, and some of the spreading functions have in fact been undersampled. From P5, transmitters suspended at 10 m (in the mixed layer), we find low spreading in frequency, comparable to the winter results. It should be noted that the difference between the P5 SD10 curves in Figs. 16a and b is due to source movements. Not all summer data have been analyzed, but from what we have seen only the shallow suspended source gives small spreading in frequency. Changing receiver depth from 40 m to 54 m does not change this. The deep suspended cases and those with the source on the bottom all cause

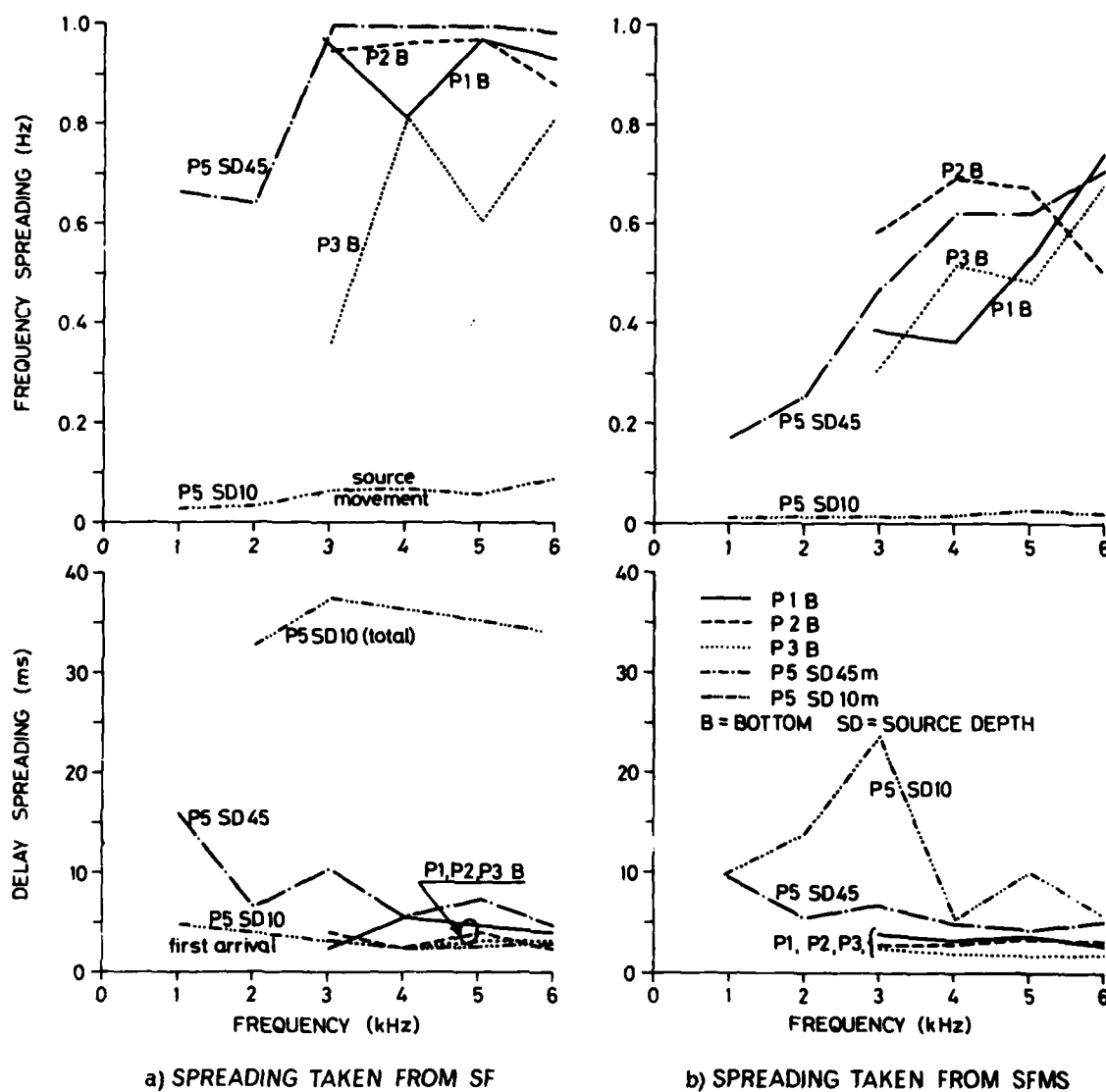


FIG. 16 SPREADING IN FREQUENCY AND DELAY, SUMMER.
 VARIABLE SOURCE LOCATION,
 POSITIONS P1, P2, P3 SOURCE DEPTH: BOTTOM.
 RECEIVER DEPTH: 54 m.
 POSITION P5 SOURCE DEPTH: 10 m and 45 m.
 RECEIVER DEPTH: 40 m.

large spreading. Time spreading of bottom runs in summer is almost the same as for winter. The result from P5, with the source at 10 m depth, is different because there are two strong and clearly separated arrivals or arrival clusters (see Fig. 16a). All other cases show one dominant (or only one) arrival/arrival cluster.

Summarizing the spreading results we note that the 3 dB time or delay spreading is generally small in most cases, near 5 ms when one arrival is dominant. Two strong arrivals lead to some 40 ms total spreading (in summer). The 3 dB frequency spreading is much more variable. However, except for some intermediate cases we can classify the results in two groups:

- 1) very small spreading, below 0.05 to 0.1 Hz
- 2) relatively large spreading ≥ 1 Hz, not resolved because of under-sampling.

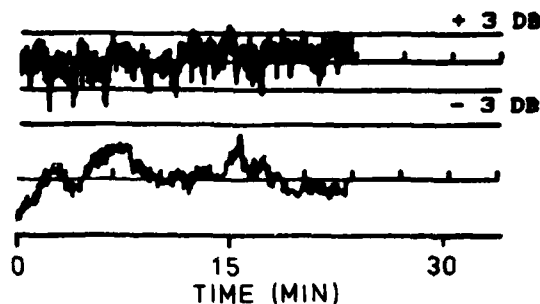
Considering the variables involved in the experiments we find that varying source location, source depth, or receiver depth do not cause changes as big as those that occur between summer and winter (as expected).

5.4 Transmission Loss and Transmission-Loss Time Variations

Transmission loss has been calculated on some of the data used in the spreading calculations. We recall that once every second a sum of linear FM sweep pulses of 125 ms length was transmitted. The energy of the received pulse has been computed for each individual frequency band. Using what we know about source level, hydrophone sensitivity, and gains, we calculated the actual transmission loss for each ping and frequency band of a run. The time length of a run has usually been 30 minutes. All signals used were 500 Hz signals symmetric around the centre frequency of transmission. The transmission-loss values given are thus averages over a nominal time length of 1/8 second and a nominal bandwidth of 500 Hz centred at the given frequency. The pulse repetition rate of 1 Hz is our sample frequency of the transmission-loss/time variations.

The curves in Figs. 17 and 18 show examples of variations with time of logarithmic transmission loss in winter and summer respectively. Mean values and standard deviations of transmission loss calculated over the run time are also given. It should be noted that we do not give the true standard deviation: the numbers presented have been derived from the logarithmic transmission-loss values and not from the linear ones. For moderate fluctuation levels this "logarithmic" standard deviation is a reasonably good approximation to the lg (true standard deviation). Note the differences in scale between the curves, indicated by the ± 3 dB lines around the mean values. We see that in most cases the major part of the time fluctuations is confined within these ± 3 dB lines. However, the fluctuation amplitudes are generally greater in summer, and the fluctuations are also much more irregular. Peaks or dips of up to 12 dB amplitude may occur. We also observe that the level of fluctuations in most cases increases with increasing centre frequency of transmission. The lowest frequency signals, 1 kHz, are clearly less variable than the others.

a)

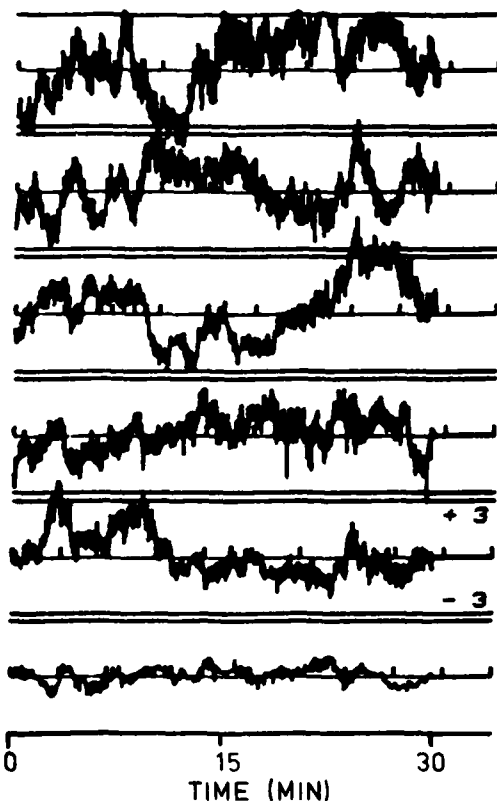


2 KHZ MEAN = 885 DB
STD.DEV. = 13 DB

POSITION P8

RANGE
38500 m

SOURCE DEPTH
45 m

TRANSMISSION LOSS
TIME VARIATIONS

6 KHZ MEAN = 872 DB
STD.DEV. = 17 DB

5 KHZ MEAN = 807 DB
STD.DEV. = 11 DB

4 KHZ MEAN = 801 DB
STD.DEV. = 15 DB

3 KHZ MEAN = 815 DB
STD.DEV. = 9 DB

2 KHZ MEAN = 776 DB
STD.DEV. = 11 DB

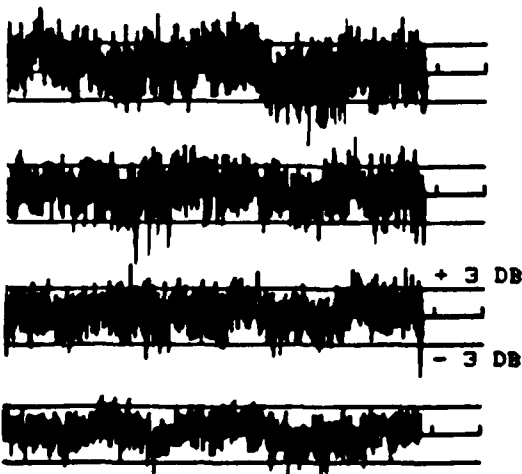
1 KHZ MEAN = 673 DB
STD.DEV. = 4 DB

b)

POSITION P5

RANGE
25500 m

SOURCE DEPTH
45 m



6 KHZ MEAN = 815 DB
STD.DEV. = 21 DB

5 KHZ MEAN = 800 DB
STD.DEV. = 18 DB

4 KHZ MEAN = 795 DB
STD.DEV. = 16 DB

3 KHZ MEAN = 845 DB
STD.DEV. = 13 DB

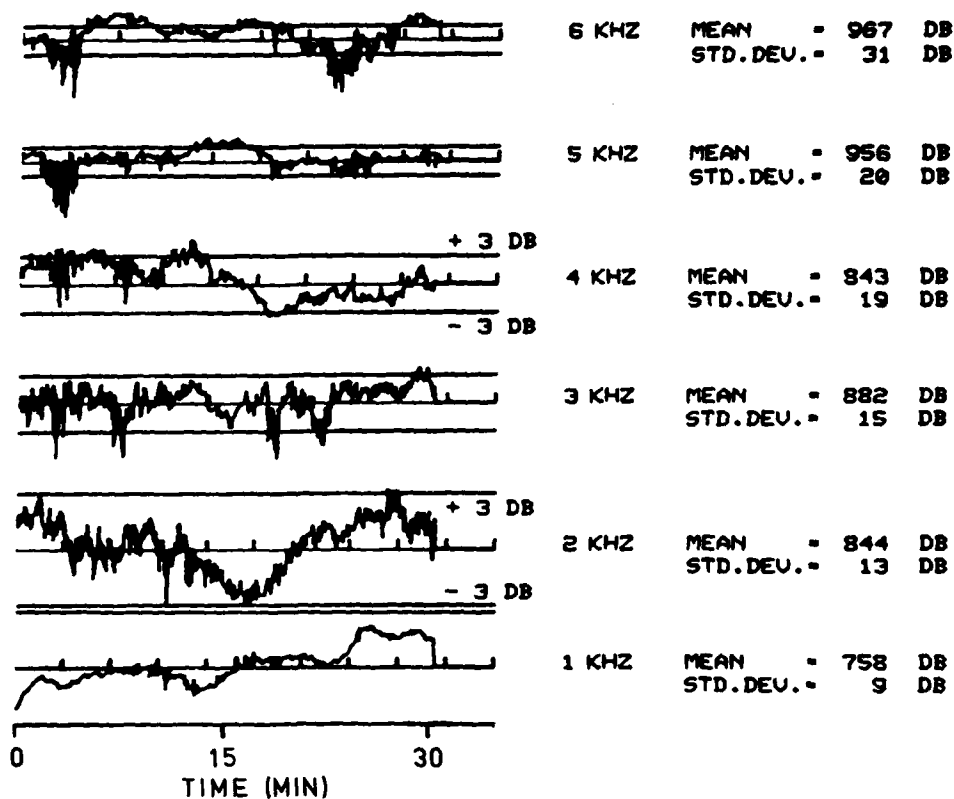
c)

POSITION P2

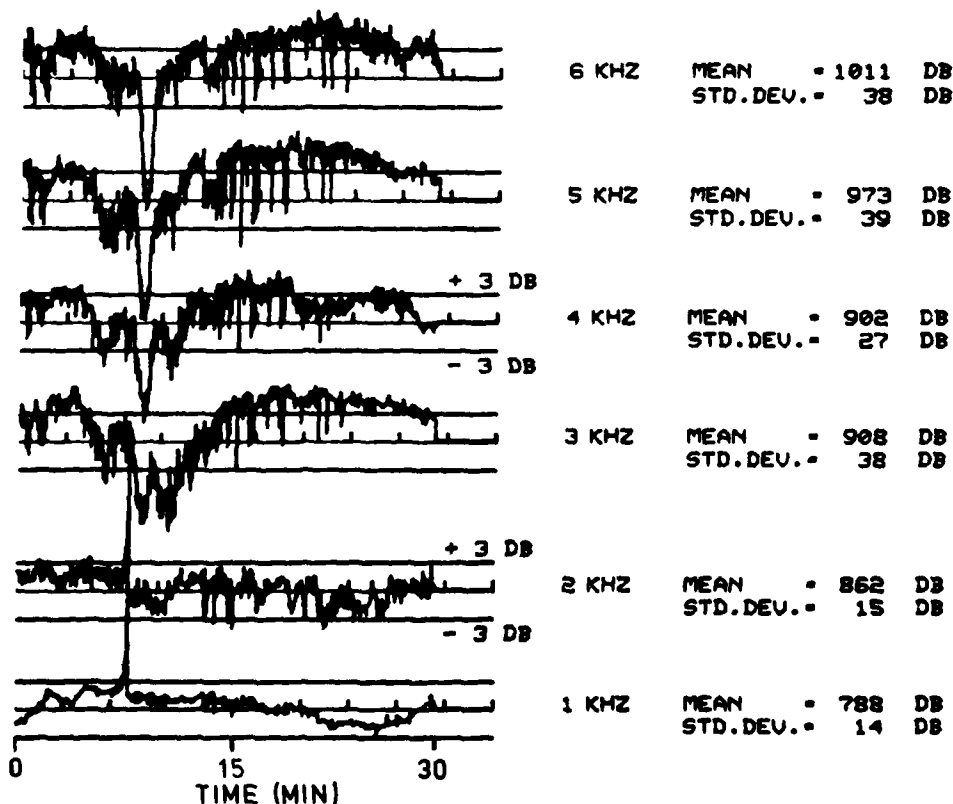
RANGE
12800 m

SOURCE DEPTH
BOTTOM

FIG. 17 TRANSMISSION-LOSS TIME VARIATIONS, WINTER 78,
POSITION P2, P5, P8, RECEIVER DEPTH 40 m



a)
SOURCE DEPTH
45 m



b)
SOURCE DEPTH
10 m

FIG. 18 TRANSMISSION-LOSS VARIATIONS, SUMMER 77,
POSITION P5, RANGE 25500 m, RECEIVER DEPTH 40 m

A bottom-mounted transducer (Fig. 17c) seems to cause rapid fluctuations of 2 to 3 dB amplitude, which creates a curve of transmission loss against time that is quite different from the rest. The example shown in Fig. 17a (range: 38.5 km) was a special one. There was a strong wind and a rough sea, and the only signal received was the 1 kHz one. Thus the 1 kHz curve shows true transmission loss, whereas the 2 kHz curve is noise only.

Figures 19, 20 and 21 display the variability of the mean transmission loss and (logarithmic) standard deviation with spatial variables and season. Figure 19a shows how the mean transmission loss varies with position and range. There seems to be only small correlation with range, which indicates that location, bottom topography, and other bottom properties are more important. Local minima around 4 kHz are a feature found very often in these TML data. It is believed to be a true effect of the medium because computer propagation model runs (see Ch. 6) quite often give a similar result. Spreading around the mean lies between 1 and 2 dB, with position P3 being the lowest. On the average, the standard deviation does not increase much with frequency. Variations of TML with receiver depth are shown in Fig. 19b. More than 10 dB difference is observed. The deepest hydrophone signal has been damped more than the others. Another deep hydrophone (95 m) shows the smallest TML, less than the two midwater-depth hydrophone signals. The mean \pm standard deviation curves have also been drawn around the two extreme mean value curves. Spreading here is not very different from that in Fig. 19a.

Figure 20 compares summer and winter results at two positions. Mean value \pm standard deviation curves are presented. We find that in these cases TML in summer is 20 dB higher than in winter. In summer at position P2 the mean TML is higher with a source in the mixed layer (10 m) than with the source on the bottom. Both positions P5 and P2 show approximately the same mean TML level even though the P2 range is only half the P5 range.

The figures also show spherical spreading plus absorption-loss curves for the two ranges. We observe that in summer the mean transmission loss is higher than predicted by spherical spreading and absorption. The winter results lie below, but are still much higher than given by cylindrical spreading. Loss in addition to that attributed to shallow-water cylindrical spreading and absorption is due to bottom interaction. Concerning spreading around the mean, the indications are for a higher standard deviation in summer than in winter.

In Fig. 21a we see variations with transducer depth at position P5 in summer. Bottom signals are more damped than signals from the mixed layer, and a midwater source gives the lowest mean TML. Spreading here is large and the curves are fairly irregular. The transmission loss variability with season is summarized in Fig. 21b where the results have been averaged over all spatial variables. The two seasonal TML curves are spaced some 10 dB at mid-frequencies, the difference being smaller at lower frequencies and greater at higher frequencies. There is an average difference in (logarithmic) standard deviation of less than 1 dB for the higher frequencies.

Summarizing the transmission-loss results, we have found that in summer the mean TML is higher than predicted by spherical spreading and absorption. Winter values are 10 dB below on the average. Bottom loss accounts for the increased mean TML relative to shallow-water cylindrical-spreading

predictions. Range is less important than location and bottom properties. Mean TML varies with source and receiver depth. The deepest source and the deepest receiver seem to cause highest loss. Quite often we observe local minima in the transmission loss curves around 4 kHz. The winter transmission-loss fluctuations are generally within ± 3 dB of the mean value.

The exceptions are not too many and the deviations not too great. In summer the ± 3 dB limit is also quite often valid but fluctuations are stronger and more irregular (Fig. 18b). Sometimes we observe strong, narrow peaks or dips in the transmission-loss curves. The amplitudes of these excursions may reach 10 to 12 dB (or even more). Strength of the fluctuations in general increases with frequency, but calculated average "logarithmic" standard deviation in summer is close to 2.5 dB over the higher part of the frequency range. This is approximately 1 dB above the average winter values.

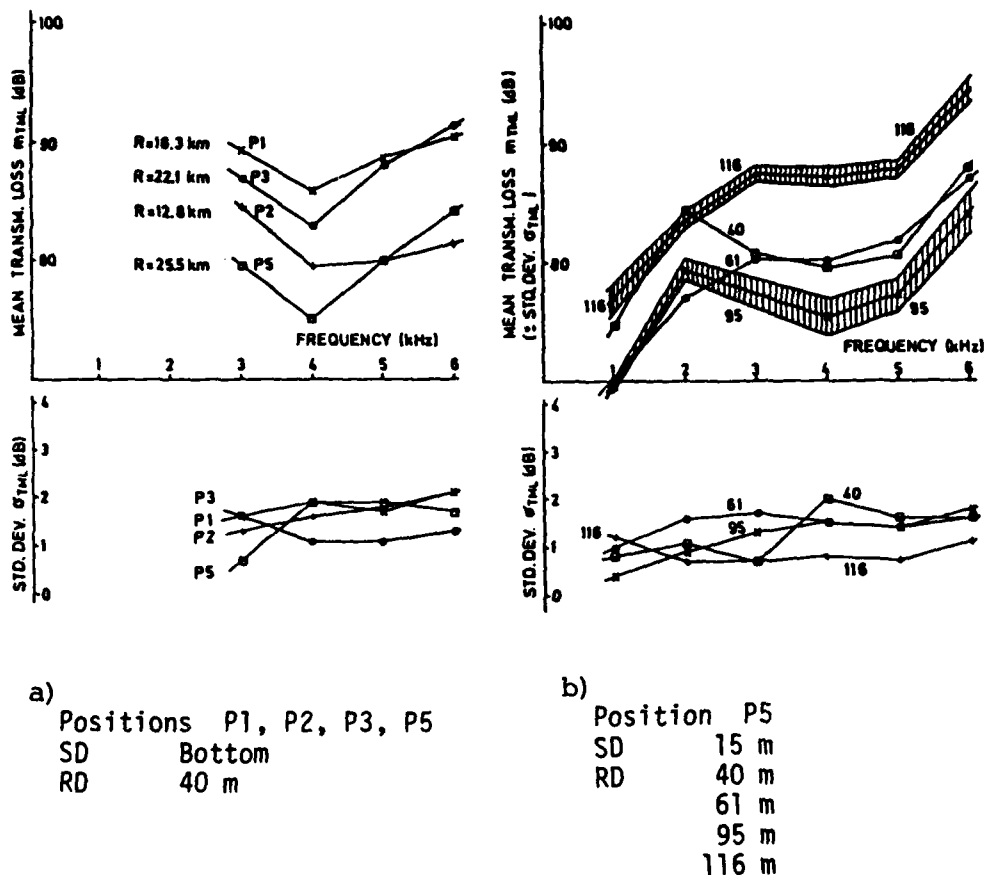


FIG. 19 TRANSMISSION-LOSS VARIABILITY WITH POSITION AND RECEIVER DEPTH

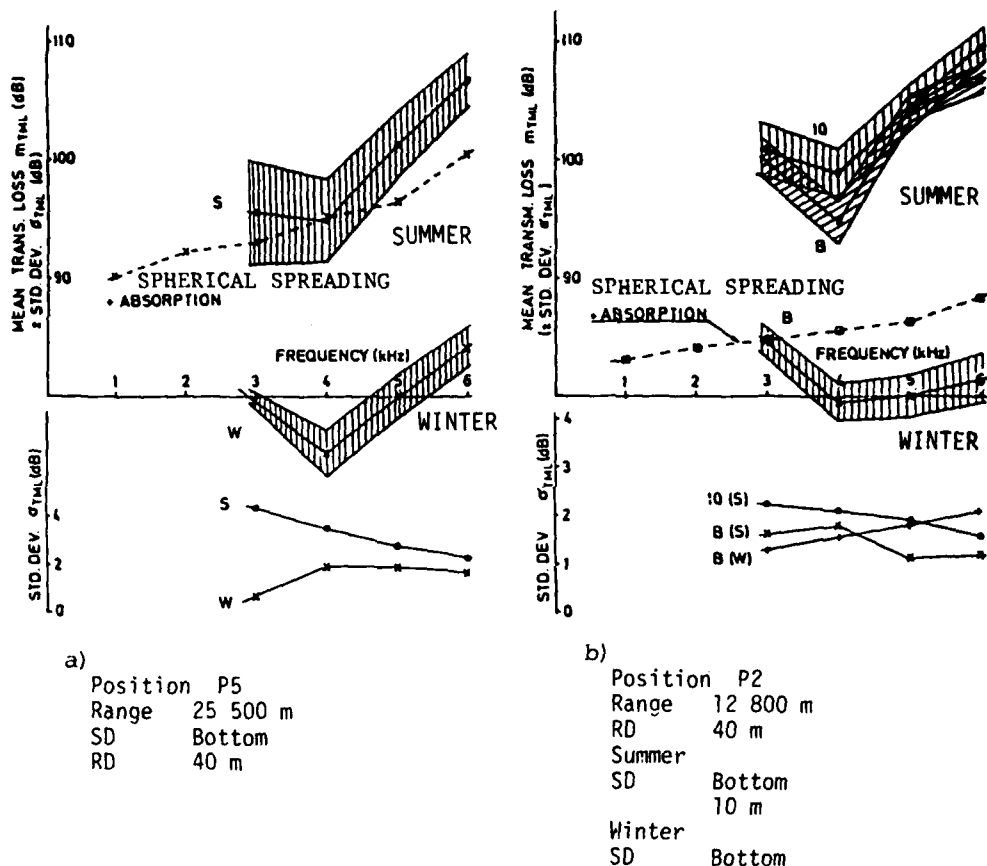


FIG. 20 TRANSMISSION-LOSS VARIABILITY, SUMMER AND WINTER

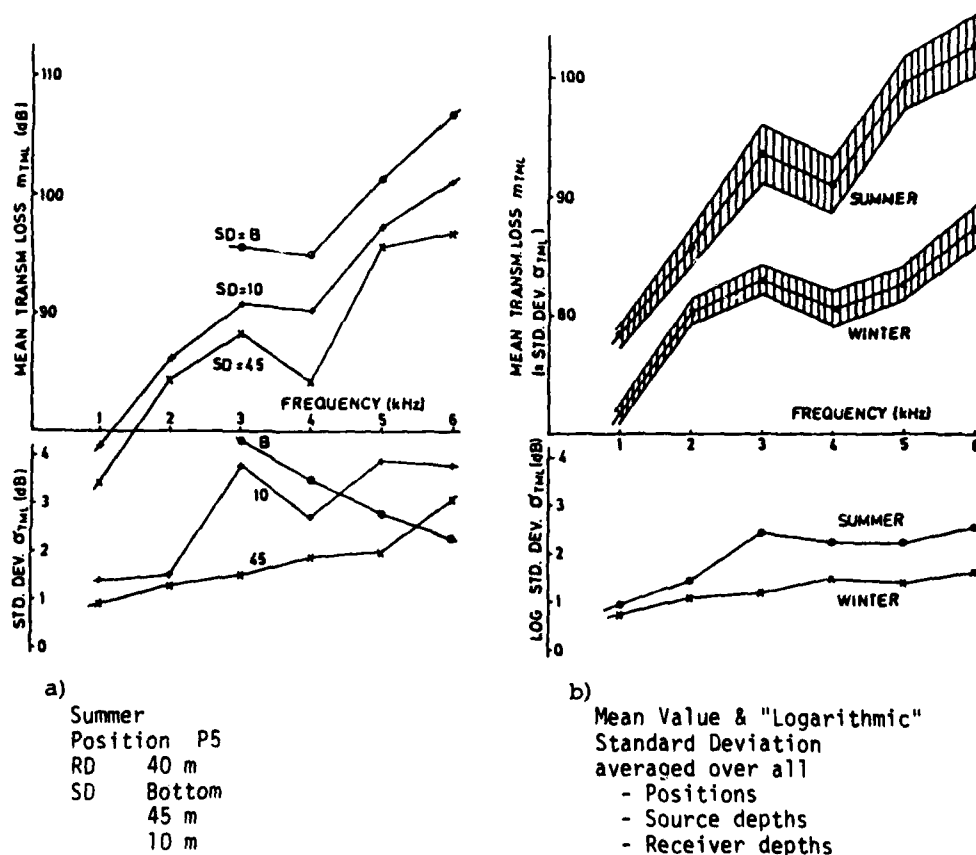


FIG. 21 TRANSMISSION-LOSS VARIABILITY WITH SOURCE DEPTH: AVERAGED OVER ALL SPATIAL VARIABLES, SUMMER AND WINTER

6 DISCUSSION

Transmission-loss calculations are based on the energy or amplitude of the received signals. Transmission-loss variation is thus a measure of amplitude fluctuation. Frequency spreading on the other hand is a measure of phase fluctuation or time coherence. Time or delay spreading provides information on the existing mode/multipath structure.

The transmission-loss results, mean values, and fluctuations around the mean, do not pose any major interpretation problems. Time or delay spreading belongs to the same category. It is generally found to be small because only one arrival is dominant. In a few cases we observe more than one strong arrival, which results in increased delay spreading (summer).

Frequency spreading is different. Except for some intermediate results we classify them in two groups, one showing very little spreading and the other much more.

We discuss first the intermediate results and the effects of surface waves. Figure 13 presented an example in which the surface-wave spectrum shows up as sidebands in the scattering-function plots.

The important fact pertaining to this run is that the transducer was bottom mounted and that the wave spectrum peaked at a low dominant frequency. It is likely that we always have this modulation effect, but it may not be visible if the source is suspended from the ship or the wave spectrum is without an LF peak. This can be seen from Figs. 14b and 15b (positions P1 and P2). The increase in frequency spreading observed is the combined effects of the medium and of source movements. The effect due to the medium is in this case thought to be primarily that of surface roughness. However, we have seen that roughness alone does not necessarily have any effect and that direction of transmission is also important. There are indications that downwind (or upwind) transmissions will cause some frequency spreading, while crosswind transmissions will not.

It is difficult to assess the relative importance of medium (surface) effects and source movements as causes of frequency spreading. Figure 8b, however, makes us think that source movements are not too important.

We have tried to minimize the spreading due to (radial) movements by weighting the frequency width of the spreading functions with the level of the spreading functions. There are indications that an increase in frequency spreading due to movements is accompanied by a decrease in the level of the spreading function. (See for example Fig. 8b, where frequency-shift changes of the spreading functions are associated with increased frequency width and reduced level).

We now turn to the two groups of significantly different frequency-spreading results. We have seen that relatively large spreading is the result of either variable shifts of the spreading functions or large widths, or both. We think that what we have observed is the combined result of propagation conditions, experimental geometry, bottom interaction, surface roughness, and internal wave action. The spreading itself is caused by internal waves and to some degree also by surface roughness.

There is reason to believe that internal-wave action in shallow water is not vertically isotropic and that internal waves will most likely be strongest around the steepest temperature or density gradients. Thus signals propagating at the depth of strongest internal-wave action, or spending most of the time there, would experience the largest spreading in frequency, i.e. the largest reduction in coherence.

It is possible that we are dealing basically with two different types of arrivals or groups of modes. One of them is a direct arrival or one that has experienced a few reflections only, which is equivalent to one or a small group of low-order mode. The other type of arrival is one that has been subjected to many surface and/or bottom reflections, i.e. a group of higher order modes. The second type of arrival would be delayed relative to the first. Unfortunately no calculations of total delay have been made. It is likely that the delayed arrivals will also be more damped than the first. Thus when both arrival types are present the first will dominate over the second. Usually the last arrival will be more spread because the travel time is longer. However, the spreading in frequency is most likely determined by where the signal carrying most of the energy propagates. So in some cases the more or less direct path will be spread most because it has propagated through the depth of strongest internal-wave action. In other cases the other type of arrival will experience more spreading because, with its many bottom or surface reflections, it passes through the depths of strong internal waves several times, thus picking up random phase changes. Given the propagation conditions and the bottom properties (source location) the source and receiver depths determine the mode or multipath structure.

From knowledge of the internal wave field it should be possible to estimate fluctuation effects at the receiver. Unfortunately we do not have this knowledge.

We now want to check if our transmission-loss calculations can help us in the interpretation of the spreading results. Since spreading functions are based on phase and transmission loss is based on amplitude, it is not to be expected that we will find any close relationship. Going back to Fig. 17 we recall that the signals in a) and b) were not much spread (coherent) while the signal in c) showed relatively large spreading in frequency. Comparing also with Fig. 19a, we see that for position P2 with the source on the bottom, neither mean TML nor spreading around the mean is significantly different from the other cases. What remains is the visual impression of the curve of transmission-loss variation with time, which is somewhat different from the other winter curves. Turning now to Fig. 18 we note that a) shows an incoherent signal while b) represent a coherent one. We see that the coherent signal is more damped and also seems to be more irregular in terms of fluctuations. In short, there seems to be very little connection between the mean value of the transmission loss and either the fluctuations around the mean or the spreading function.

To gain further insight into the processes involved and as a control of our calculated transmission-loss values we have used two computer propagation models. One was GRASS <15>, a range-dependent ray-trace model that accepts a segmented range. The other was SNAP <16>, a normal-mode model that includes slight range dependence in the environmental parameters (adiabatic approximation); it accepts segmented inputs in depth, sound-speed profile, and bottom parameters. For the models to produce correct results it is

necessary for the set of environmental input parameters to the models to be correct and complete.

The model runs are compared with experimental results in Figs. 22 to 25. In terms of transmission loss the overall impression is that the models compare quite well with experimental winter data.

Modelling summer conditions is more difficult. Differences are generally greater, and GRASS usually gave the better predictions. SNAP quite often predicted too high loss, see for instance Figs. 22b and c. Figure 22c also displays one notable exception. For position P5 and source depth at 45 m, both models and the experimental results follow each other closely. At a source depth of 10 m, on the other hand, results are quite different. SNAP should be more accurate than GRASS provided that a good set of input data is available. It is likely that the set of bottom parameters used in the computations is incomplete since it is in summer, when bottom interaction is strongest, that SNAP fails most. Bottom parameters from the position P8 range are well known. We see from Fig. 22a that the agreement between SNAP and experiment is very good at 1 kHz for this range both in summer and winter. The 2 kHz results are out of agreement because of a very low signal-to-noise ratio in the experimental data.

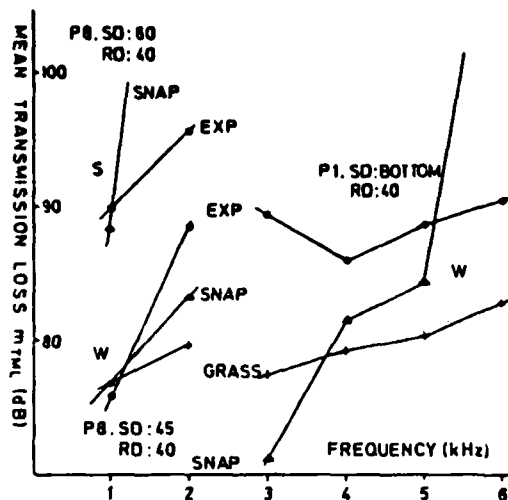
Figure 23 displays ray-tracings from GRASS in summer (the ray-tracings from winter are not presented because they show very little). We recall that in summer a shallow source produced coherent signals (small spreading) at the receiver while a deep source resulted in coherence reduction (large spreading). We observe from Figs. 23a and b that there seems to be more energy at the 40 m and 54 m hydrophone depths when the source is at 10 m than when it is on the bottom. This at least makes it likely that the received signals could be more coherent in the first case than in the second. The paths involved in both cases are bottom-reflected-refracted. It should be noted, however, that measured mean transmission loss is about equal in the two cases. Figure 23c shows ray tracings from position P1 with the source at 45 m. Results from the experiments indicate that the received signals in this case should be incoherent. From the figure we observe that signals at the 40 m and 54 m hydrophone depth are rather strong and that the paths involved are largely refracted.

This could mean coherent received signals. On the other hand if there is strong internal-wave action at the depth of the refracted paths this would work in the opposite direction. Of course the GRASS output is sensitive to the accuracy of the sound-speed values inputted. Judging from the prevailing summer propagation conditions there should be no sound channel at P1. Unfortunately no spreading-function calculations were done on data from this run.

Figures 24 and 25 show outputs from the SNAP normal-mode model. The individual plots display mode energy versus arrival angle or mode number. Results are shown for three frequencies from four different cases. In both figures a) represents a case found to be incoherent and b) represents a coherent case. From the figures we observe that the energy seems to be concentrated on fewer modes in the coherent case and that these modes are clustered together in something we could call a mode group. In the coherent bottom case, Fig. 24b, we also observe one strong low-order mode in two cases. If most of the energy is carried by one such mode the received signal will most likely be coherent.

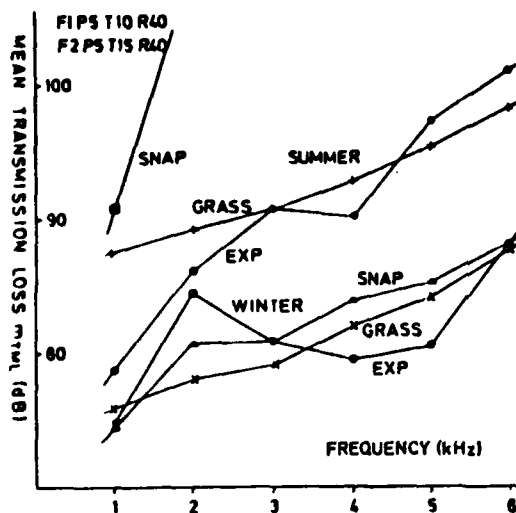
Our model runs have not provided us with any conclusive evidence concerning the interpretation of the spreading results. The reasons why the models fail to solve our problems can be summed up as follows:

- The environmental input parameter set has been incomplete. This applies to sound-speed variations in space and time (both models) and bottom parameters (SNAP).
- Ray tracing implies equal propagation conditions for all frequencies. The SNAP model works on a single frequency, that of the centre frequency of transmission. Signals used during the experiments were fixed bandwidth, 500 Hz signals centred at frequencies from 1 kHz to 6 kHz.
- Neither GRASS nor SNAP contain any element of time variability of the input parameters. The sound-speed profile at a certain location is assumed to remain constant with time. Thus effects of internal waves will not be seen. Only different conditions leading to differences in these effects might be observed.



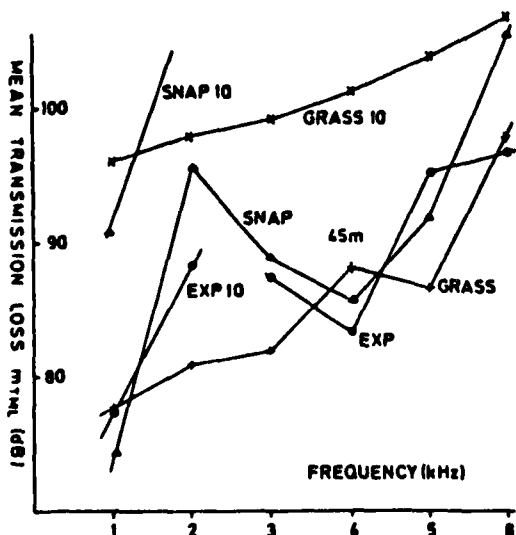
a)

Position	P8	Position	P1
RD	40 m	RD	40 m
Summer		SD	Bottom
SD	60 m	Winter	
Winter			
SD	45 m		



b)

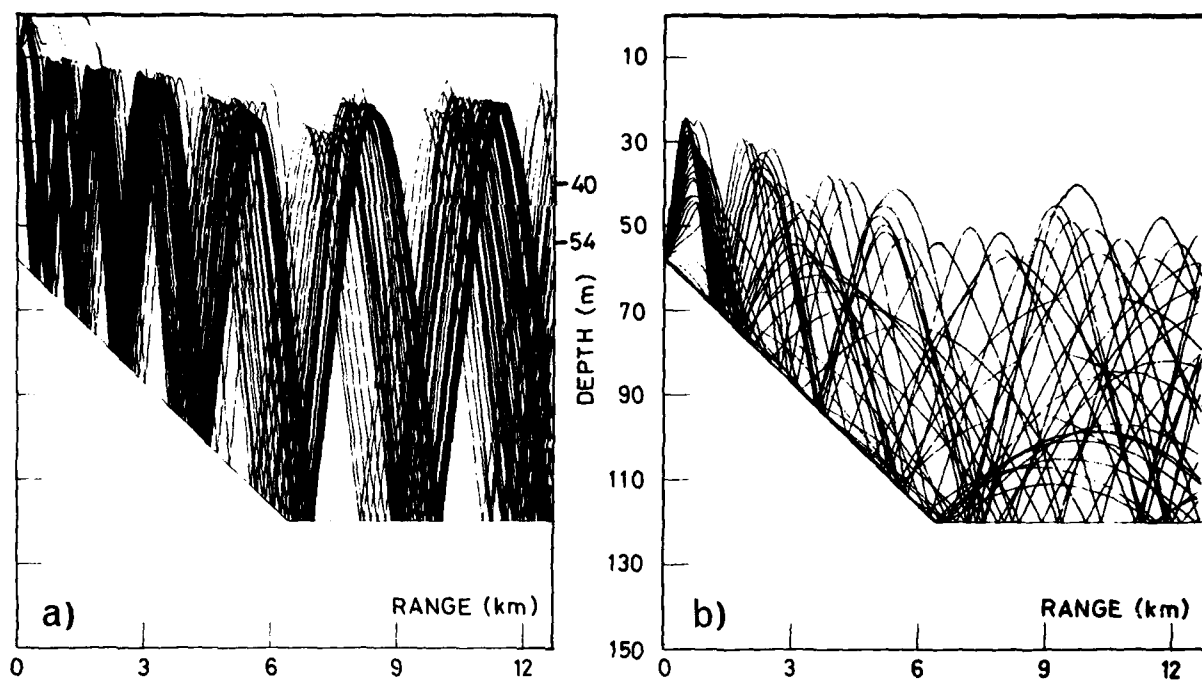
Position	P5
RD	40 m
Summer	
SD	10 m
Winter	
SD	15 m



c)

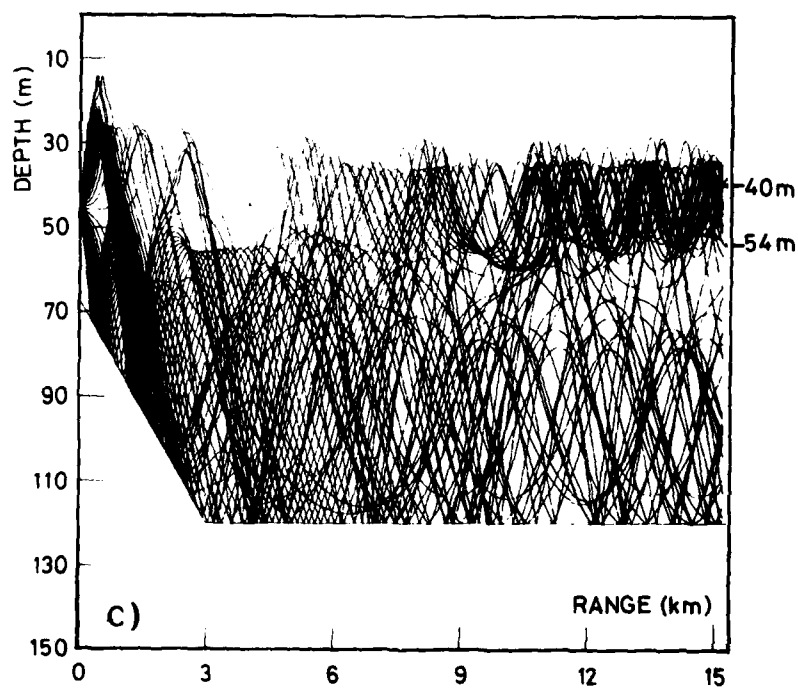
Position	P5
RD	54 m
SD	10 m
	45 m
Summer	

FIG. 22 TRANSMISSION LOSS: COMPARISON BETWEEN MODELS AND EXPERIMENT



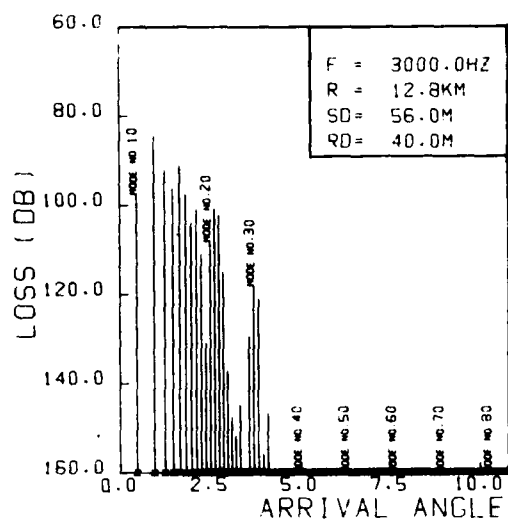
POSITION P2 SOURCE DEPTH: 10 m

POSITION P2 SOURCE DEPTH : BOTTOM

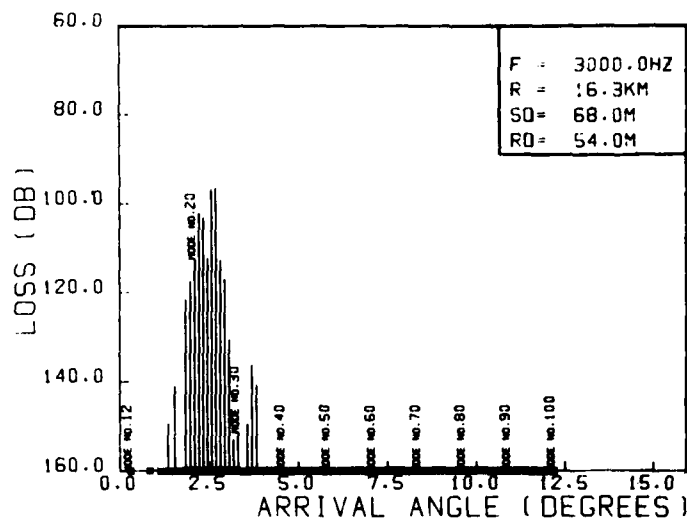


POSITION P1 SOURCE DEPTH: 45 m

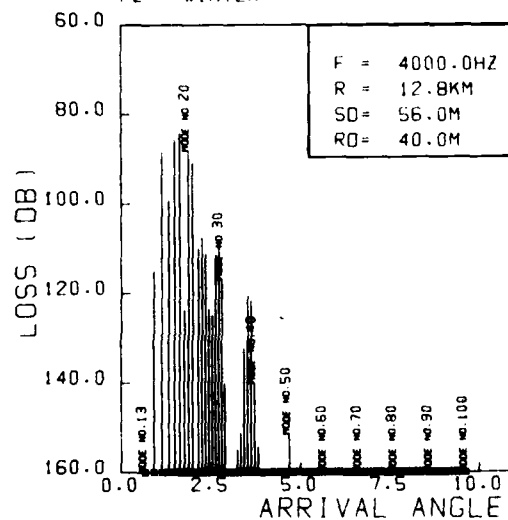
FIG. 23 RAY TRAYCINGS (GRASS), SUMMER 77, POSITIONS 1 and 2



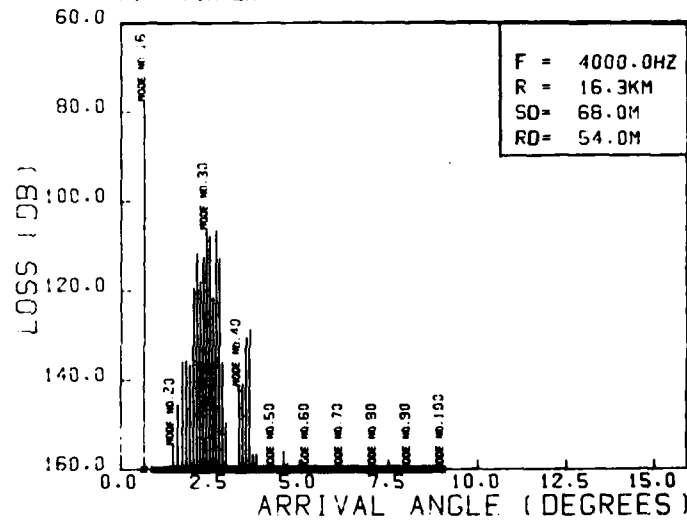
P2 - WINTER



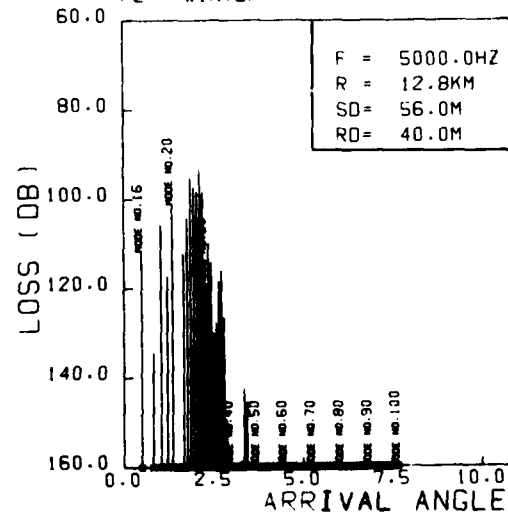
P1 - WINTER



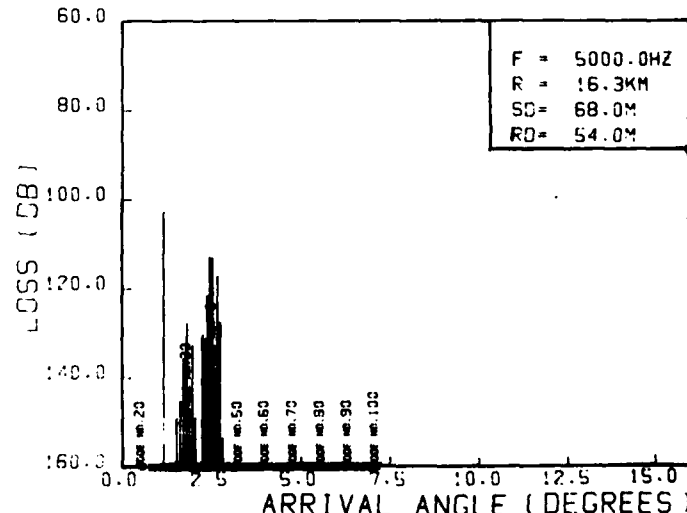
P2 - WINTER



P1 - WINTER



P2 - WINTER

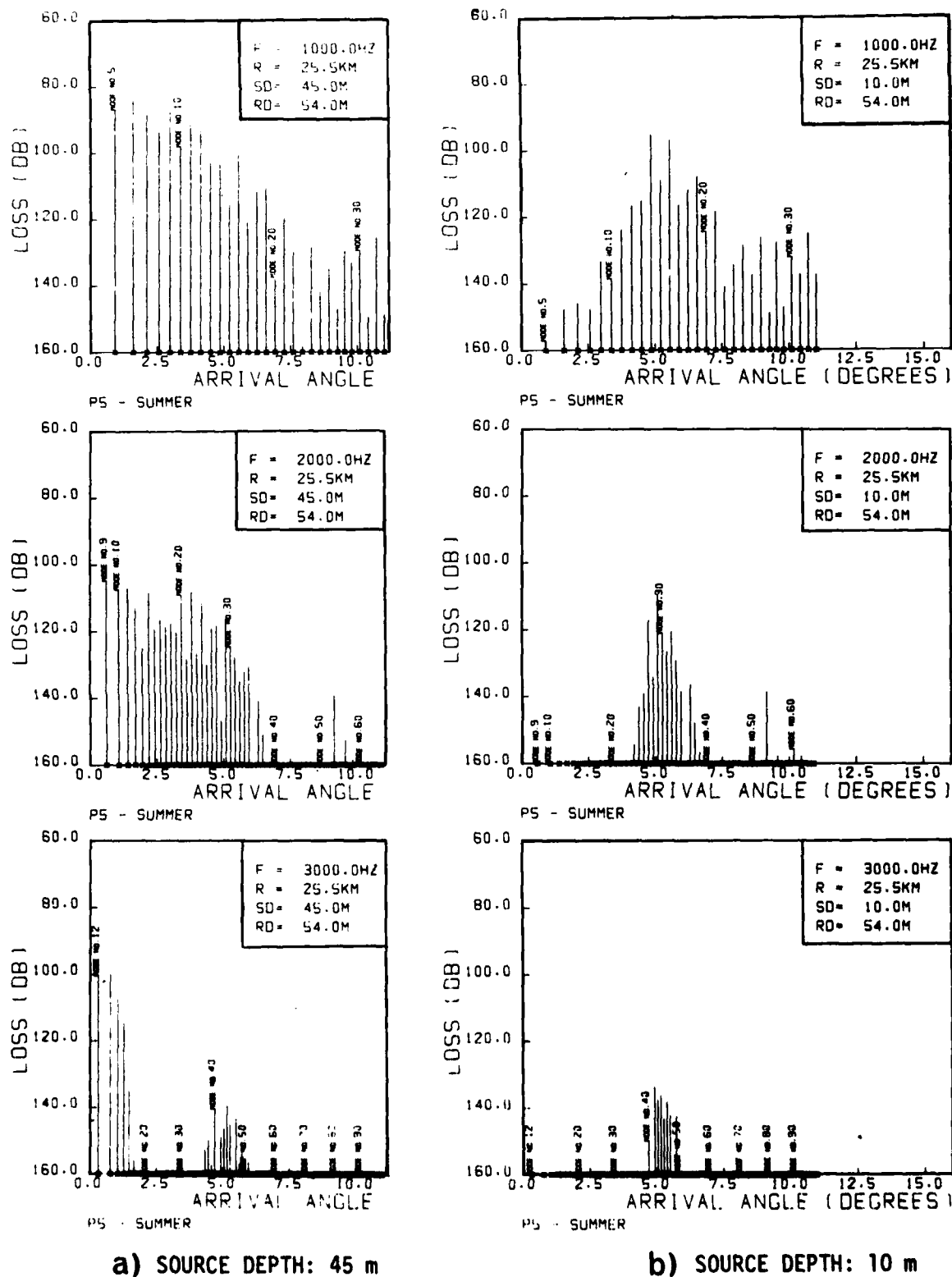


P1 - WINTER

a) POSITION P2
RECEIVER DEPTH 40 m

b) POSITION P1
RECEIVER DEPTH 54 m

FIG. 24 SNAP MODE-ENERGY vs ARRIVAL ANGLE, WINTER 78
SOURCE DEPTH: BOTTOM



CONCLUSIONS

We have studied the effects of a fluctuating medium on signals propagating through the medium. These fluctuations are visible as surface roughness but, more important, they also exist in the water masses as internal waves. The effects of these time variations in the medium on signals passing through are to impose amplitude and phase fluctuations on the signals. Signal phase fluctuations have been observed as (varying) widths in frequency of the spreading functions (or scattering functions) of the medium. Amplitude fluctuations that manifest themselves as changes in level and/or duration of the received signals have been observed as transmission-loss variations and variations in time length of the spreading functions. The averaging time has been the duration of an individual experiment, usually 30 minutes.

We have found that the statistical processes involved cannot in general be considered stationary. Thus the scattering function concept is strictly not valid. However, in comparison with those from spreading functions, the scattering function results have turned out to be meaningful in most cases. Indications are also that the mechanisms causing frequency-spreading variations are different from those causing variations in delay spreading and transmission loss.

Variables associated with the experiments have been

- time/season (summer and winter)
- centre frequency of transmission (1, 2, 3, 4, 5 and 6 kHz)
- space (five source locations, three source depths and - except in one case - two receiver depths).

The biggest changes occur when we go from one season to the other; this was to be expected since this involves the biggest changes in the sound-propagation conditions. Mean summer transmission loss is on the average some 10 dB above the winter values. Fluctuations of transmission loss are usually within ± 3 dB of the mean value. Conditions are more irregular in summer than in winter, and peaks and dips of up to 12 dB amplitude may occur. Delay or time spreading lies around 5 ms, with some exceptions in summer where we observe more than one strong arrival (arrival cluster). Frequency spreading also changes with season. However, it is not the numerical value of the spreading but the relative importance of the variables that change.

Centre frequency of transmission is not so important, but we observe some local transmission-loss minima at 4 kHz. Mean transmission loss and fluctuations around the mean generally show some increase with frequency. Delay spreading is constant with frequency or may sometimes show some decrease. Frequency spreading seems to be quite constant with frequency in most low-spread cases. High spreading involves undersampling and very little can be said about frequency dependence. Among the intermediate cases we observe several with frequency spreading increasing strongly with centre frequency of transmissions. The cause of spreading in these cases is thought to be interaction with the sea surface. Undersampling sometimes creates an artificial increase in frequency spreading with frequency of transmission (summer).

Variations with location can be quite large. We note that source-to-receiver range is less important than bottom properties. The depth of the source or receiver can also be important but there seems to be no clear trend.

The frequency-spreading results are the most difficult to interpret. Except for some intermediate cases the results can be classified in two groups, one with small spreading, Δf_e (0.05 to 0.1 Hz), the other undersampled with a spreading Δf of more than 1 Hz. We think that what we have observed is the combined result of propagation conditions, bottom properties, surface waves, and internal wave action. However, due to lack of environmental data it has not been possible to model the situation and to prove that this is indeed a complete explanation. For this purpose we would need a much more complete sampling of the variations of sound speed with time and space and this would also provide information on the internal-wave field.

We also need to know more about the bottom composition in general. To make predictions of average signal levels in the frequency range of 1 to 6 kHz it should be sufficient to know the bottom parameters in the upper few metres of the sediments. To be able to predict fluctuations around the mean values we need a model that incorporates time variations in the propagation conditions.

ACKNOWLEDGEMENTS

Underwater Research Division

F. Jensen: running the SNAP model
on environmental data

S. Mari: transfer and digitization of data

A. Legner: data analysis and illustrations

Real-Time Systems Dept.

R. Seynaeve

Electronic Engineering Dept.

A. Barbagelata

REFERENCES

1. GARRETT, C. and MUNK, W. Internal waves in the ocean. Annual Review of Fluid Mechanics, 1979: 339-369.
2. Flatté S.M., ed., Sound Transmission through a Fluctuating Ocean. London, Cambridge University Press, 1979.
3. DESAUBIES, Y.J.F. Acoustic fluctuations in the ocean. In: LANTERBORN, W., ed. Cavitation and Inhomogeneities in Underwater Acoustics, Proceedings of the First International Conference, Göttingen, Federal Republic of Germany, 9-11 July, 1979. Berlin, Springer, 1980: 281-293.
4. BELLO, P.A. Characterization of randomly time-variant linear channels. IEEE Transactions on Communications Systems, 1963: 360-393.
5. ELLINTHORPE, A.W. and NUTTALL, A.H. Theoretical and Empirical Results on the Characterization of Undersea Acoustic Channels, TR-65-8-BF. Waltham, Mass., Litton Systems Inc., 1977. [AD 631 620]
6. SØSTRAND, K.A. Mathematics of the time-varying channel. In: NATO Advanced Study Institute on Signal Processing with Emphasis on Underwater Acoustics, Proceedings, 12-23 August, 1968. Enschede, Twente Institute of Technology, 1968: 25/1-25/20.
7. LAVAL, R. Sound propagation effects on signal processing. In: GRIFFITHS, J.W.R., STOCKLIN, P.L. and SCHOONEVELD, C. VAN., eds. Signal Processing. Proceedings of the NATO Advanced Study Institute on Signal Processing with Particular Reference to Underwater Acoustics, held at Loughborough, England, under the Auspices of the Loughborough University of Technology. London, Academic Press, 1973: 223-241.
8. DE FERRARI, H.A. and LAN NGHIEM-PHU. Scattering function measurements for a 7-NM propagation range in the Florida Straits. Journal of the Acoustical Society of America, 1974: 47-52.
9. COSTA, D. and HUG, E. An estimation of the scattering function of an undersea acoustic channel. Alta Frequenza, 45, 1976: 241-245.
10. LAVAL, R. Time-frequency space generalized coherence and scattering functions. In: TACCONI, G., ed. Aspects of Signal Processing with Emphasis on Underwater Acoustics, Part 1. Proceedings of the NATO Advanced Study Institute held at Portovenere, La Spezia, Italy, 30 August - 11 September, 1976. Dordrecht, The Netherlands, 1977: 69-87.
11. FRAZER, M.E. Some statistical properties of lake surface reverberation. Journal of the Acoustical Society of America, 64, 1978: 858-868.
12. JOBST, W.J. and ADAMS, S.L. Statistical analysis of ambient noise. Journal of the Acoustical Society of America, 62, 1977: 63-71.

13. ARASE, T. and ARASE, E.M. Deep-sea ambient noise statistics. Journal of the Acoustical Society of America, 44, 1968: 1679-1684.
14. FISZ, M. Probability Theory and Mathematical Statistics, 3rd edn. New York, N.Y., Wiley, 1963.
15. CORNYN, J.J. GRASS, a digital-computer ray-tracing and transmission-loss-prediction system, Pt 1: Overall description, NRL Rpt 7621, Pt 2: User's manual, NRL Rpt 7642. Washington, DC, US Naval Research Laboratory, 1973.
16. JENSEN, F. and FERLA, M.C. SNAP: the SACLANTCEN normal-mode acoustic propagation model, SACLANTCEN SM-121. La Spezia, Italy, SACLANT ASW Research Centre, 1979. [AD AO 672 256]

ADDITIONAL BIBLIOGRAPHY

- ANDREWS, R.S. and TURNER, L.F. Investigation of the amplitude fluctuations of high-frequency short-duration sound pulses propagated under short-range shallow-water conditions. Journal of the Acoustical Society of America, 58, 1975: 331-335.
- PRESTON, J. and NISLEY, R. Simple frequency modulation model for surface reflection of a CW tone. Journal of the Acoustical Society of America, 64, 1978: 601-604.
- ZORNIG, J.G. Physical model studies of forward surface scatter frequency spreading. Journal of the Acoustical Society of America, 64, 1978: 1492-1499.
- JOBST, W. and DOMINIJANNI, L. Measurements of the temporal, spatial, and frequency stability of an underwater acoustic channel. Journal of the Acoustical Society of America, 65, 1979: 62-69.
- BOEHME, H. Measurements of acoustic backscattering from very rough water surfaces. Journal of the Acoustical Society of America, 65, 1979: 350-359.
- ANDREWS, R.S. Forward scattering of underwater sound and its frequency dependence on the medium. Journal of the Acoustical Society of America, 65, 1979: 672-674.

SACLANTCEN SR-46

INITIAL DISTRIBUTION

<u>MINISTRIES OF DEFENCE</u>		<u>SCNR FOR SACLANTCEN</u>
MOD Belgium	2	SCNR Belgium
DND Canada	10	SCNR Canada
CHOD Denmark	8	SCNR Denmark
MOD France	8	SCNR Germany
MOD Germany	15	SCNR Greece
MOD Greece	11	SCNR Italy
MOD Italy	10	SCNR Netherlands
MOD Netherlands	12	SCNR Norway
CHOD Norway	10	SCNR Portugal
MOD Portugal	5	SCNR Turkey
MOD Turkey	5	SCNR U.K.
MOD U.K.	16	SCNR U.S.
SECDEF U.S.	61	SECGEN Rep. SCNR
		NAMILCOM Rep. SCNR
<u>NATO AUTHORITIES</u>		<u>NATIONAL LIAISON OFFICERS</u>
Defence Planning Committee	3	NLO Canada
NAMILCOM	2	NLO Denmark
SACLANT	10	NLO Germany
SACLANTREPEUR	1	NLO Italy
CINWESTLANT/COMOCEANLANT	1	NLO U.K.
COMIBERLANT	1	NLO U.S.
CINCEASTLANT	1	
COMSUBACLANT	1	
COMNAIREASTLANT	1	
SACEUR	2	
CINCNORTH	1	
CINCSOUTH	1	
COMNAVSOUTH	1	
COMSTRIKFORSOUTH	1	
COMEDCENT	1	
COMNAIRARMED	1	
CINCHAN	1	

Total initial distribution
SUGGESTED LIBRARY
STUDY
